

A New Scalar Auxiliary Variable Approach for Gradient Flows

Jinpeng Zhang^a, Xiaoping Wang^{b,c,*}

^a*Department of Mathematics, University of Macau, Macao SAR, China*

^b*School of Science and Engineering, The Chinese University of Hong Kong, Shenzhen, Guangdong 518172, China & Shenzhen International Center for Industrial and Applied Mathematics, Shenzhen Research Institute of Big Data, Guangdong 518172, China*

^c*Department of Mathematics, the Hong Kong University of Science and Technology, Hong Kong, China*

Abstract

The scalar auxiliary variable (SAV) approach [1] is a highly efficient method widely used for solving gradient flow systems. This approach offers several advantages, including linearity, unconditional energy stability, and ease of implementation. By introducing scalar auxiliary variables, a modified system that is equivalent to the original system is constructed at the continuous level. However, during temporal discretization, computational errors can lead to a loss of equivalence and accuracy. In this paper, we introduce a new Constant Scalar Auxiliary Variable (CSAV) approach in which we derive an Ordinary Differential Equation (ODE) for the constant scalar auxiliary variable r . We also introduce a stabilization parameter (α) to improve the stability of the scheme by slowing down the dynamics of r . The CSAV approach provides additional benefits as well. We explicitly discretize the auxiliary variable in combination with the nonlinear term, enabling the solution of a single linear system with constant coefficients at each time step. This new approach also eliminates the need for assumptions about the free energy potential, removing the bounded-from-below restriction imposed by the nonlinear free energy potential in the original SAV approach. Finally, we validate the proposed method through extensive numerical simulations, demonstrating its effectiveness and accuracy.

Keywords: Scalar auxiliary variable (SAV), Energy stable, Gradient flows, Phase field models

1. Introduction

The gradient flow systems, which conform to the second law of thermodynamics, are widely used as models in various scientific and engineering fields, including materials science and fluid dynamics [2, 3, 4, 5, 6, 7]. When the total free energy is known, the gradient flow model can be derived based on the dissipation mechanism and the

*Corresponding author: wangxiaoping@cuhk.edu.cn

variation of free energy. In this paper, we consider a free energy given by

$$E(\phi) = \int_{\Omega} \frac{1}{2} \phi \mathcal{L} \phi + F(\phi) d\Omega, \quad (1)$$

where Ω represents the spatial domain, \mathcal{L} is a linear self-adjoint elliptic operator, and $F(\phi)$ is the free energy density, a nonlinear function. The corresponding gradient flow system for the above free energy is then formulated as

$$\begin{cases} \phi_t = -\mathcal{G}\mu, \\ \mu = \frac{\delta E(\phi)}{\delta \phi} = \mathcal{L}\phi + F'(\phi), \end{cases} \quad (2)$$

with either periodic boundary conditions or the homogeneous Neumann boundary condition $\frac{\partial \phi}{\partial \mathbf{n}} \partial \Omega = \frac{\partial \mu}{\partial \mathbf{n}} \partial \Omega = 0$, where \mathbf{n} denotes the outward normal of $\partial \Omega$. Moreover, \mathcal{G} is a semi-positive definite operator known as the mobility operator and μ is the chemical potential. The triplet $(\phi, \mathcal{G}, E(\phi))$ uniquely determines the gradient flow system. For instance, by taking $\mathcal{G} = 1$ and $E(\phi) = \int_{\Omega} \frac{\epsilon^2}{2} |\nabla \phi|^2 + \frac{1}{4} (\phi^2 - 1)^2 d\Omega$, where ϵ is a model parameter, we obtain the well-known Allen-Cahn equation introduced by Samuel M. Allen and John W. Cahn in [8]

$$\phi_t = -\mu = \epsilon^2 \Delta \phi - (\phi^3 - \phi). \quad (3)$$

Similarly, considering $\mathcal{G} = -\Delta$ and $E(\phi) = \int_{\Omega} \frac{\epsilon^2}{2} |\nabla \phi|^2 + \frac{1}{4} (\phi^2 - 1)^2 d\Omega$, we arrive at the Cahn-Hilliard equation introduced by John W. Cahn and John E. Hilliard in [9]

$$\phi_t = \Delta \mu, \quad (4)$$

$$\mu = -\epsilon^2 \Delta \phi + (\phi^3 - \phi). \quad (5)$$

Furthermore, for $\mathcal{G} = 1$ and $E(\phi) = \int_{\Omega} \frac{\epsilon^2}{2} (\Delta \phi)^2 + \frac{1}{4} (|\nabla \phi|^2 - 1)^2 d\Omega$, we obtain the molecular beam epitaxy model with slope selection [10]

$$\phi_t = -\mu = -\epsilon^2 \Delta^2 \phi + \nabla \cdot ((|\nabla \phi|^2 - 1) \nabla \phi). \quad (6)$$

All the aforementioned models satisfy the following energy law

$$\frac{d}{dt} E(\phi) = - \int_{\Omega} \frac{\delta E(\phi)}{\delta \phi} \mathcal{G} \frac{\delta E(\phi)}{\delta \phi} d\Omega \leq 0, \quad (7)$$

provided that the boundary terms are canceled.

When designing numerical schemes for gradient flow models, there are two main challenges: handling the nonlinear terms $F(\phi)$ and ensuring that the numerical algorithms preserve the energy dissipation law at the discrete level. In recent years, several popular numerical algorithms have been developed to address these challenges. One approach is the convex splitting approach [11, 12, 13], which leads to a convex minimization problem at each time step, ensuring

unconditional energy stability. However, it requires solving a nonlinear system at each time step, and designing second-order unconditionally energy stable convex splitting schemes is not possible in a general manner. Second-order convex splitting schemes can only be constructed on a case-by-case basis. Another approach is the stabilized linearly implicit approach [14, 15], which addresses the nonlinear terms explicitly and incorporates additional regularization terms to relax the strict constraints on the time step. However, it is typically limited to first-order accuracy. The exponential time differencing (ETD) approach [16, 17] achieves high-order accuracy by integrating the governing equation over a single time step and using polynomial interpolations for the nonlinear terms. However, there is still a lack of theoretical proof for the energy stability properties of high-order ETD schemes. The invariant energy quadratization (IEQ) approach [18, 19] can result in unconditionally energy stable, linear, second-order schemes for a wide range of gradient flow systems. However, it requires solving a coupled linear system with variable coefficients at each time step and assumes that the free energy density $F(\phi)$ is bounded from below.

As a remedy, the Scalar Auxiliary Variable (SAV) approach was proposed in [20, 1]. It introduces scalar auxiliary variables instead of auxiliary function variables and a modified system that is mathematically equivalent to the original gradient flow system at the continuous level. The SAV approach retains the advantages of the IEQ approach and only assumes that the free energy $\int_{\Omega} F(\phi)d\Omega$ is bounded from below. It requires solving only two linear systems with constant coefficients at each time step. However, errors generated during numerical calculations can lead to a loss of this equivalence relationship (this problem will be explained in detail in the next section). One possible remedy for this is to use adaptive time stepping strategies [21, 22]. A Lagrange multiplier approach was introduced in [23] to enforce dissipation of the original energy. Recently, a relaxed Scalar Auxiliary Variable (RSAV) approach and its generalized version (R-GSAV) were introduced in [24, 25]. The idea is to add a relaxation step to the original SAV approach in order to improve the consistency between the original system and the modified system, while retaining all the advantages of SAV. This method involves solving the modified system at each time step and addressing the inconsistency between the modified energy and the original energy through an optimization problem. The computational cost associated with this optimization problem is negligible. However, it does not guarantee that the solved modified system is equivalent to the original system during numerical computation, resulting in inaccurate original energy in the optimization problem.

In [26], an Exponential Scalar Auxiliary (E-SAV) approach was introduced, which defines an exponential form of the auxiliary variable, offering several advantages. It removes the bounded-from-below restriction of the nonlinear free energy potential and provides a fully explicit discretization of the auxiliary variable combined with the nonlinear term. Consequently, it only needs to solve one linear system with constant coefficients at each time step.

In [27], the authors developed a novel fully-decoupled numerical technique (DSAV) to solve the variable-density/viscosity Cahn-Hilliard phase-field model of the binary-phase incompressible fluid flow system. Utilizing the so-called “zero-

energy-contribution” feature, they introduced two nonlocal variables and design two special ordinary differential equations (ODEs) for them, which are trivial on the continuous level. A linear, unconditionally energy stable and fully-decoupled scheme is then constructed. This DSAV method is generalized to the droplet formation problem which is modeled by Cahn- Hilliard-Navier-Stokes equations with a non-homogeneous Dirichlet boundary conditions in [28].

In this paper, we propose a new method called the Constant Scalar Auxiliary Variable (CSAV) method. This method introduces a new constant scalar auxiliary variable r and incorporates a stabilization parameter α to enhance accuracy and stability. The introduction of a small parameter α aims to slow down the change of the constant scalar variable, ensuring consistency between the original system and the modified system after numerical discretization, without the need to decrease the time step size. The CSAV method offers greater efficiency and flexibility compared to the original SAV method. The advantages of the CSAV method can be outlined as follows:

- It effectively resolves the inconsistency problem between the original system and the modified system.
- It does not require any assumptions, unlike the original SAV approach that assumes the nonlinear free energy function $\int_{\Omega} F(\phi)d\Omega$ to be bounded from below.
- It only requires solving one linear system with constant coefficients, whereas the SAV approach requires solving two linear systems. As a result, the computational cost of the CSAV method is essentially half that of the SAV approach.

The remainder of this paper is organized as follows. In Section 2, we revisit the original SAV method and the relaxed SAV (RSAV) method for general gradient flow systems. Subsequently, we propose our new method, the constant SAV (CSAV) method. We rigorously prove the energy stability properties of the CSAV method in Section 3. Then, in Section 4, we demonstrate how the CSAV approach can be easily applied to gradient flows of various functions. Section 5 presents specific examples and numerical tests to verify the accuracy and effectiveness of the proposed constant SAV numerical schemes. Finally, we conclude with a brief summary.

2. A brief review of the original SAV and relaxed SAV methods

Consider the general gradient flow system described by the following equations:

$$\phi_t = -\mathcal{G}\mu, \tag{8}$$

$$\mu = \frac{\delta E(\phi)}{\delta \phi} = \mathcal{L}\phi + f(\phi), \tag{9}$$

Here, ϕ represents the state variable, $E(\phi)$ is the free energy, and \mathcal{G} is a semi-positive definite operator for gradient flow systems. We assume a simplified form of the free energy $E(\phi) = \int_{\Omega} (\frac{1}{2}\phi\mathcal{L}\phi + F(\phi))d\Omega$, where \mathcal{L} is a linear self-adjoint elliptic operator, $F(\phi)$ is the bulk free energy density, and $f(\phi)$ is the derivative of $F(\phi)$. The system is subject to either periodic boundary conditions or $\frac{\partial\phi}{\partial\mathbf{n}}|_{\partial\Omega} = \frac{\partial\mu}{\partial\mathbf{n}}|_{\partial\Omega} = 0$, where \mathbf{n} denotes the outward normal of $\partial\Omega$. For simplicity, we consider periodic boundary conditions in this paper.

By taking the L^2 inner product of the first equation (8) with μ and the second equation (9) with ϕ_t , we immediately obtain the energy dissipation law:

$$\frac{d}{dt}E(\phi) = - \int_{\Omega} \mu\mathcal{G}\mu d\Omega. \quad (10)$$

When \mathcal{G} is semi-positive definite, we have $\frac{d}{dt}E(\phi) \leq 0$, indicating energy dissipation in the system.

2.1. The original SAV method

Let $E_0(\phi) = \int_{\Omega} (F(\phi) - \frac{s}{2}\phi^2)d\Omega$, and assume $E_0(\phi) + C_0 > 0$, where $C_0 > 0$ is a constant. Here, s is a regularization parameter first introduced in [29]. The key idea of the original Scalar Auxiliary Variable (SAV) method is to introduce a scalar auxiliary variable $q(t) = \sqrt{E_0(\phi) + C_0}$ and expand the original system (4)-(5) into the following equivalent system,

$$\phi_t = -\mathcal{G}\mu, \quad (11)$$

$$\mu = \mathcal{L}\phi + s\phi + \frac{q(t)}{\sqrt{E_0(\phi) + C_0}}(f(\phi) - s\phi), \quad (12)$$

$$q_t = \frac{1}{2\sqrt{E_0(\phi) + C_0}} \int_{\Omega} (f(\phi) - s\phi)\phi_t d\Omega. \quad (13)$$

For this modified system, the modified energy E_M is denoted as:

$$E_M(\phi) = \int_{\Omega} (\frac{1}{2}\phi\mathcal{L}\phi + \frac{1}{2}s\phi^2)d\Omega + q^2 - C_0. \quad (14)$$

This modified energy also satisfies the energy law, and its rigorous proof is provided in [20, 1]. Instead of discretizing the original system (4)-(5), we can discretize the modified system (11)-(13).

Consider the time domain $[0, T]$ and discretize it into equally spaced meshes $0 = t_0 < t_1 < \dots < t_N = T$, where $t_i = i\Delta t$ and $\Delta t = T/N$. Let ψ^n represent the numerical approximation to the function $\psi(\cdot, t)|_{t=tn}$. Using these notations, a first-order SAV-BDF semi-discrete scheme for (11)-(13) can be constructed as follows:

$$\frac{\phi^{n+1} - \phi^n}{\delta t} = -\mathcal{G}\mu^{n+1}, \quad (15)$$

$$\mu^{n+1} = \mathcal{L}\phi^{n+1} + s\phi^{n+1} + \frac{q^{n+1}}{\sqrt{E_0(\phi^n) + C_0}}(f(\phi^n) - s\phi^n), \quad (16)$$

$$\frac{q^{n+1} - q^n}{\delta t} = \int_{\Omega} \frac{(f(\phi^n) - s\phi^n)}{2\sqrt{E_0(\phi^n) + C_0}} \frac{\phi^{n+1} - \phi^n}{\delta t} d\mathbf{x}, \quad (17)$$

It can be easily shown that the above scheme is unconditionally energy stable [20, 1]. Similarly, a second-order SAV-CN semi-discrete scheme can be obtained as follows:

$$\frac{\phi^{n+1} - \phi^n}{\delta t} = -\mathcal{G}\mu^{n+\frac{1}{2}}, \quad (18)$$

$$\mu^{n+\frac{1}{2}} = \mathcal{L}\phi^{n+\frac{1}{2}} + s\phi^{n+\frac{1}{2}} + \frac{q^{n+\frac{1}{2}}}{\sqrt{E_0(\bar{\phi}^{n+\frac{1}{2}}) + C_0}} \left(f(\bar{\phi}^{n+\frac{1}{2}}) - s\bar{\phi}^{n+\frac{1}{2}} \right), \quad (19)$$

$$\frac{q^{n+1} - q^n}{\delta t} = \int_{\Omega} \frac{\left(f(\bar{\phi}^{n+\frac{1}{2}}) - s\bar{\phi}^{n+\frac{1}{2}} \right)}{2\sqrt{E_0(\bar{\phi}^{n+\frac{1}{2}}) + C_0}} \frac{\phi^{n+1} - \phi^n}{\delta t} d\mathbf{x}, \quad (20)$$

where $\phi^{n+\frac{1}{2}} = \frac{1}{2}(\phi^n + \phi^{n+1})$ and $\bar{\phi}^{n+\frac{1}{2}} = \frac{3}{2}\phi^n - \frac{1}{2}\phi^{n-1}$. This numerical scheme is also unconditionally energy stable, and its rigorous proof can be found in [20, 1].

2.2. The relaxed SAV method

The relaxed SAV (RSAV) method was proposed in [24]. The idea is to introduce a relaxation step to the original SAV approach to improve the consistency between the original system and the modified system. Taking the second-order RSAV-CN numerical scheme as an example, its numerical scheme is as follows:

Step 1. Calculate the intermediate solution $(\phi^{n+1}, \tilde{q}^{n+1})$ using the original SAV-CN method as shown below:

$$\frac{\phi^{n+1} - \phi^n}{\Delta t} = -\mathcal{G}\mu^{n+\frac{1}{2}}, \quad (21)$$

$$\mu^{n+\frac{1}{2}} = \mathcal{L}\phi^{n+\frac{1}{2}} + s\phi^{n+\frac{1}{2}} + \frac{\tilde{q}^{n+1} + q^n}{2\sqrt{E_0(\bar{\phi}^{n+\frac{1}{2}}) + C_0}} \left(f(\bar{\phi}^{n+\frac{1}{2}}) - s\bar{\phi}^{n+\frac{1}{2}} \right), \quad (22)$$

$$\frac{\tilde{q}^{n+1} - q^n}{\Delta t} = \int_{\Omega} \frac{\left(f(\bar{\phi}^{n+\frac{1}{2}}) - s\bar{\phi}^{n+\frac{1}{2}} \right)}{2\sqrt{E_0(\bar{\phi}^{n+\frac{1}{2}}) + C_0}} \frac{\phi^{n+1} - \phi^n}{\delta t} d\mathbf{x}. \quad (23)$$

Step 2. Update the scalar auxiliary variable q^{n+1} through a relaxation step as follows:

$$q^{n+1} = \xi_0 \tilde{q}^{n+1} + (1 - \xi_0) \sqrt{E_0(\phi^{n+1}) + C_0}, \quad \xi_0 \in \mathcal{V}, \quad (24)$$

where the feasible set \mathcal{V} is defined as:

$$\mathcal{V} = \left\{ \xi \in [0, 1] \mid (q^{n+1})^2 - (\tilde{q}^{n+1})^2 \leq \Delta t \eta \left(\mathcal{G}\mu^{n+\frac{1}{2}}, \mu^{n+\frac{1}{2}} \right), \quad q^{n+1} = \xi \tilde{q}^{n+1} + (1 - \xi) \sqrt{E_0(\phi^{n+1}) + C_0} \right\}. \quad (25)$$

Here, $\eta \in [0, 1]$ is an artificial parameter that can be manually assigned.

Remark (Optimal choice for ξ_0): Now we explain the optimal choice for the relaxation parameter ξ_0 . We can determine ξ_0 as the solution of the following optimization problem:

$$\xi_0 = \min_{\xi \in [0, 1]} \xi, \quad \text{s.t.} \quad (q^{n+1})^2 - (\tilde{q}^{n+1})^2 \leq \Delta t \eta \left(\mu^{n+\frac{1}{2}}, \mathcal{G}\mu^{n+\frac{1}{2}} \right).$$

This can be simplified as

$$\xi_0 = \min_{\xi \in [0,1]} \xi, \quad \text{s.t. } a\xi^2 + b\xi + c \leq 0,$$

where the coefficients are

$$\begin{aligned} a &= \left(\tilde{q}^{n+1} - \sqrt{E_0(\phi^{n+1}) + C_0} \right)^2, \quad b = 2 \left(\tilde{q}^{n+1} - \sqrt{E_0(\phi^{n+1}) + C_0} \right) \sqrt{E_0(\phi^{n+1}) + C_0}, \\ c &= (E_0(\phi^{n+1}) + C_0) - (\tilde{q}^{n+1})^2 - \Delta t \eta \left(\mu^{n+\frac{1}{2}}, \mathcal{G} \mu^{n+\frac{1}{2}} \right). \end{aligned}$$

Given $a \neq 0$, the solution to (3.13) is given as

$$\xi_0 = \max \left\{ 0, \frac{-b - \sqrt{b^2 - 4ac}}{2a} \right\}$$

The numerical scheme given by equations (21)-(24) is unconditionally energy stable, and its rigorous proof can be found in [24].

In this approach, the solution ϕ^{n+1} is obtained by solving a modified system in Step 1 and then using this solution to solve the optimization problem in Step 2. Therefore, it is crucial to ensure that the discretized modified system in Step 1 is equivalent to the original system. This means that the term $\frac{\tilde{q}^{n+1} + q^n}{2\sqrt{E_0(\tilde{\phi}^{n+\frac{1}{2}}) + C_0}}$ in equation (22) should be close to 1. If this term deviates from 1, it indicates that the solution ϕ^{n+1} is inaccurate, which can negatively impact the overall accuracy of the method.

3. The constant SAV approach for gradient flows

In the original SAV method, we have $\frac{q(t)}{\sqrt{E_0(\phi) + C_0}} = 1$. Therefore the original system (4)-(5) and the modified system (11)-(13) are equivalent at continuous level. However, after temporal discretization, the numerical values of $q(t)$ and $\sqrt{E_0(\phi) + C_0}$ may no longer be equal, indicating that the two systems may not remain equivalent.

Multiply (13) with $q(t)$, we have

$$(q(t)^2)_t = \frac{q(t)}{\sqrt{E_0(\phi) + C_0}} \int_{\Omega} (f(\phi) - s\phi) \phi_t d\Omega. \quad (26)$$

By the definition of $q(t)$, we can obtain

$$(E_0(\phi) + C_0)_t = (q(t))^2_t = \int_{\Omega} (f(\phi) - s\phi) \phi_t d\Omega. \quad (27)$$

After temporal discretization, this identity no longer holds due to discretization errors. That is,

$$\frac{(E_0(\phi^{n+1}) + C_0) - (E_0(\phi^n) + C_0)}{\Delta t} \neq \frac{(q^{n+1})^2 - (q^n)^2}{\Delta t} = \int_{\Omega} (f(\phi^n) - s\phi^n) \frac{\phi^{n+1} - \phi^n}{\Delta t} d\Omega, \quad (28)$$

$$\Rightarrow E_0(\phi^{n+1}) + C_0 \neq (q^{n+1})^2, \quad (29)$$

$$\Rightarrow \frac{q^{n+1}}{\sqrt{E_0(\phi^{n+1}) + C_0}} \neq 1. \quad (30)$$

In order to reduce errors resulting from numerical calculations, we will define a new scalar auxiliary variable in the following:

$$r(t) = \frac{q(t)}{\sqrt{E_0(\phi) + C_0}} = 1 \quad (31)$$

$$\Rightarrow r(t)\sqrt{E_0(\phi) + C_0} = q(t) \quad (32)$$

Differentiating both sides of the equation (32) with respect to t . We can obtain

$$\frac{dr(t)}{dt} \sqrt{E_0(\phi) + C_0} + r(t) \frac{\int_{\Omega} (f(\phi) - s\phi)\phi_t d\Omega}{2\sqrt{E_0(\phi) + C_0}} = \frac{dq(t)}{dt} = \frac{\frac{dE_0(\phi)}{dt}}{2\sqrt{E_0(\phi) + C_0}} \quad (33)$$

$$\Rightarrow \frac{dr(t)}{dt} = \frac{(\frac{dE_0}{dt} - r(t) \int_{\Omega} (f(\phi) - s\phi)\phi_t d\Omega)}{2(E_0(\phi) + C_0)} \quad (34)$$

Because $\frac{dE_0}{dt} - r(t) \int_{\Omega} (f(\phi) - s\phi)\phi_t d\Omega = 0$, we can multiply any function on the right side of the equation (34), and the equation will still hold. Multiplying the right hand side of the equation (34) by $\beta = -2\alpha(E_0(\phi) + C_0)$, we have

$$\frac{dr}{dt} = \alpha \left(-\frac{dE_0}{dt} + r \int_{\Omega} (f(\phi) - s\phi)\phi_t d\Omega \right) \quad (35)$$

Therefore, we let $r(t)$ satisfy the following ordinary differential equation.

$$\begin{cases} \frac{dr}{dt} = \alpha \left(-\frac{dE_0}{dt} + r \int_{\Omega} (f(\phi) - s\phi)\phi_t d\Omega \right), \\ r(t)|_{t=0} = 1. \end{cases} \quad (36)$$

where α is usually taken to be very small so that the right hand side of (36) is small enough. Consequently, the value of r will be close to 1. Therefore, we can reformulate the system (4)-(5) into the following equivalent form:

$$\phi_t = -\mathcal{G}\mu, \quad (37)$$

$$\mu = \mathcal{L}\phi + s\phi + r(f(\phi) - s\phi), \quad (38)$$

$$\frac{dr}{dt} = \alpha \left(-\frac{dE_0(\phi)}{dt} + r \int_{\Omega} (f(\phi) - s\phi)\phi_t d\Omega \right). \quad (39)$$

where $E_0(\phi) = \int_{\Omega} (F(\phi) - \frac{s}{2}\phi^2) d\Omega$.

Remark.

1. The right hand side of (39) is zero at the continuous level. This allows us to multiply an arbitrarily small parameter α which can significantly slow down the change of r so that it is close to 1 (but without changing the time scale of the dynamics of ϕ) with a better control of the stability of the scheme.
2. Unlike the original SAV formulation, we don't require the nonlinear free energy function E_0 to be bounded from below in (37)-(39).

3. The system (37)-(39) can be considered as a relaxed version of the Lagrange multiplier approach introduced in [23]. However, in [23], one needs to solve a nonlinear algebraic equation for the Lagrange multiplier. As we will see later, we can design a simple, explicit (for nonlinear term) linear scheme with constant coefficient for our system (37)-(39).

Theorem 1. The modified system (37)-(39) satisfies the following dissipative energy law

$$\frac{d}{dt}E_{CM}(\phi) = - \int_{\Omega} \mu \mathcal{G} \mu d\Omega, \quad (40)$$

where

$$E_{CM}(\phi) = \frac{1}{2} \int_{\Omega} \phi \mathcal{L} \phi d\Omega + \int_{\Omega} F(\phi) d\Omega + \frac{r}{\alpha}. \quad (41)$$

Proof : By taking the inner product of (37) with μ in the L^2 space, we can get

$$\int_{\Omega} \phi_t \mu d\Omega = - \int_{\Omega} \mu \mathcal{G} \mu d\Omega. \quad (42)$$

By taking the L^2 inner product of (38) with ϕ_t , we obtain

$$\int_{\Omega} \phi_t \mu d\Omega = \frac{1}{2} \frac{d}{dt} \int_{\Omega} \phi \mathcal{L} \phi d\Omega + \frac{s}{2} \frac{d}{dt} \int_{\Omega} |\phi|^2 d\Omega + r \int_{\Omega} (f(\phi) - s\phi) \phi_t d\Omega. \quad (43)$$

By combining (42) and (43), we derive

$$\frac{1}{2} \frac{d}{dt} \int_{\Omega} \phi \mathcal{L} \phi d\Omega + \frac{s}{2} \frac{d}{dt} \int_{\Omega} |\phi|^2 d\Omega + r \int_{\Omega} (f(\phi) - s\phi) \phi_t d\Omega = - \int_{\Omega} \mu \mathcal{G} \mu d\Omega. \quad (44)$$

By multiplying (39) with $\frac{1}{\alpha}$, we obtain

$$\frac{1}{\alpha} \frac{dr}{dt} + \frac{dE_0(\phi)}{dt} = r \int_{\Omega} (f(\phi) - s\phi) \phi_t d\Omega. \quad (45)$$

By combining (45) and (44), we get

$$\frac{1}{2} \frac{d}{dt} \int_{\Omega} \phi \mathcal{L} \phi d\Omega + \frac{s}{2} \frac{d}{dt} \int_{\Omega} |\phi|^2 d\Omega + \frac{1}{\alpha} \frac{dr}{dt} + \frac{dE_0(\phi)}{dt} = - \int_{\Omega} \mu \mathcal{G} \mu d\Omega. \quad (46)$$

Using the definition of $E_0(\phi)$, $E_0(\phi) = \int_{\Omega} (F(\phi) - \frac{s}{2} \phi^2) d\Omega$, we can derive

$$\frac{dE_0(\phi)}{dt} = \frac{d}{dt} \int_{\Omega} F(\phi) d\Omega - \frac{s}{2} \frac{d}{dt} \int_{\Omega} |\phi|^2 d\Omega \quad (47)$$

By combining (47) and (46), we can get

$$\frac{1}{2} \frac{d}{dt} \int_{\Omega} \phi \mathcal{L} \phi d\Omega + \frac{d}{dt} \int_{\Omega} F(\phi) d\Omega + \frac{1}{\alpha} \frac{dr}{dt} = - \int_{\Omega} \mu \mathcal{G} \mu d\Omega. \quad (48)$$

Remark. It is worth noting that $E_{CM}(\phi)$ and the original energy $E(\phi)$ in equation (1) are equivalent, differing only by a constant.

$$E_{CM}(\phi) - E(\phi) = \frac{r}{\alpha}, \quad (49)$$

3.1. Numerical Scheme

In this section, we construct a semi-implicit first-order backward differentiation formulas (BDF) scheme, a second-order BDF2 scheme, and a second-order Crank-Nicolson (CN) scheme for the above system. Additionally, we provide a proof that all of these schemes are unconditionally energy stable.

3.2. The first-order BDF scheme

We first consider the following semi-implicit first-order BDF scheme:

$$\frac{\phi^{n+1} - \phi^n}{\Delta t} = -\mathcal{G}\mu^{n+1}, \quad (50)$$

$$\mu^{n+1} = \mathcal{L}\phi^{n+1} + s\phi^{n+1} + r^n(f(\phi^n) - s\phi^n), \quad (51)$$

$$\frac{r^{n+1} - r^n}{\Delta t} = \alpha \left(-\frac{E_0(\phi^{n+1}) - E_0(\phi^n)}{\Delta t} + r^n \int_{\Omega} (f(\phi^n) - s\phi^n) \frac{\phi^{n+1} - \phi^n}{\Delta t} d\Omega \right). \quad (52)$$

Theorem 2. The first-order scheme (50)-(52) for the equivalent system (37)-(39) is unconditionally energy stable in the sense that

$$E_{CM}^{n+1} - E_{CM}^n \leq -\Delta t \int_{\Omega} \mu^{n+1} \mathcal{G}\mu^{n+1} d\Omega - \frac{1}{2} \int_{\Omega} (\phi^{n+1} - \phi^n) \mathcal{L}(\phi^{n+1} - \phi^n) d\Omega \leq 0, \quad (53)$$

where the modified discrete version of the energy is defined by

$$E_{CM}^n = \frac{1}{2} \int_{\Omega} \phi^n \mathcal{L}\phi^n d\Omega + \frac{1}{\alpha} r^n + \int_{\Omega} F(\phi^n) d\Omega \quad (54)$$

Proof : We take the L^2 inner product of (50) with $\Delta t \mu^{n+1}$ to obtain

$$\int_{\Omega} (\phi^{n+1} - \phi^n) \mu^{n+1} d\Omega = -\Delta t \int_{\Omega} \mu^{n+1} \mathcal{G}\mu^{n+1} d\Omega. \quad (55)$$

By taking the L^2 inner product of (51) with $(\phi^{n+1} - \phi^n)$, we obtain

$$\begin{aligned} \int_{\Omega} (\phi^{n+1} - \phi^n) \mu^{n+1} d\Omega &= \frac{1}{2} \int_{\Omega} (\phi^{n+1} \mathcal{L}\phi^{n+1} - \phi^n \mathcal{L}\phi^n + (\phi^{n+1} - \phi^n) \mathcal{L}(\phi^{n+1} - \phi^n)) d\Omega \\ &+ \frac{s}{2} \left(\int_{\Omega} |\phi^{n+1}|^2 - |\phi^n|^2 + |\phi^{n+1} - \phi^n|^2 \right) d\Omega + r^n \int_{\Omega} (f(\phi^n) - s\phi^n) (\phi^{n+1} - \phi^n) d\Omega \end{aligned} \quad (56)$$

By combining (55) and (56), we can get

$$\begin{aligned} \frac{1}{2} \int_{\Omega} (\phi^{n+1} \mathcal{L}\phi^{n+1} - \phi^n \mathcal{L}\phi^n + (\phi^{n+1} - \phi^n) \mathcal{L}(\phi^{n+1} - \phi^n)) d\Omega &+ \frac{s}{2} \left(\int_{\Omega} |\phi^{n+1}|^2 - |\phi^n|^2 + |\phi^{n+1} - \phi^n|^2 \right) d\Omega \\ + r^n \int_{\Omega} (f(\phi^n) - s\phi^n) (\phi^{n+1} - \phi^n) d\Omega &= -\Delta t \int_{\Omega} \mu^{n+1} \mathcal{G}\mu^{n+1} d\Omega. \end{aligned} \quad (57)$$

By multiplying (52) with $\frac{\Delta t}{\alpha}$, we obtain

$$\frac{1}{\alpha}(r^{n+1} - r^n) + (E_0(\phi^{n+1}) - E_0(\phi^n)) = r^n \int_{\Omega} (f(\phi^n) - s\phi^n)(\phi^{n+1} - \phi^n) d\Omega \quad (58)$$

By combining (57) and (58)

$$\begin{aligned} & \frac{1}{2} \int_{\Omega} (\phi^{n+1} \mathcal{L}\phi^{n+1} - \phi^n \mathcal{L}\phi^n + (\phi^{n+1} - \phi^n) \mathcal{L}(\phi^{n+1} - \phi^n)) d\Omega + \frac{s}{2} \int_{\Omega} (|\phi^{n+1}|^2 - |\phi^n|^2 + |\phi^{n+1} - \phi^n|^2) d\Omega \\ & + \frac{1}{\alpha}(r^{n+1} - r^n) + (E_0(\phi^{n+1}) - E_0(\phi^n)) = -\Delta t \int_{\Omega} \mu^{n+1} \mathcal{G}\mu^{n+1} d\Omega. \end{aligned} \quad (59)$$

Using the definition of $E_0(\phi^{n+1})$, $E_0(\phi^{n+1}) = \int_{\Omega} (F(\phi^{n+1}) - \frac{s}{2} |\phi^{n+1}|^2) d\Omega$, we can get

$$\begin{aligned} & \frac{1}{2} \int_{\Omega} (\phi^{n+1} \mathcal{L}\phi^{n+1} - \phi^n \mathcal{L}\phi^n + (\phi^{n+1} - \phi^n) \mathcal{L}(\phi^{n+1} - \phi^n)) d\Omega + \frac{1}{\alpha} r^{n+1} - \frac{1}{\alpha} r^n + \int_{\Omega} F(\phi^{n+1}) d\Omega \\ & - \int_{\Omega} F(\phi^n) d\Omega + \frac{s}{2} \int_{\Omega} |\phi^{n+1} - \phi^n|^2 d\Omega = -\Delta t \int_{\Omega} \mu^{n+1} \mathcal{G}\mu^{n+1} d\Omega. \end{aligned} \quad (60)$$

3.3. The second-order Crank-Nicolson (CN) Scheme

We consider the following second order CN scheme:

$$\frac{\phi^{n+1} - \phi^n}{\Delta t} = -\mathcal{G}\mu^{n+\frac{1}{2}}, \quad (61)$$

$$\mu^{n+\frac{1}{2}} = \mathcal{L}\phi^{n+\frac{1}{2}} + s\phi^{n+\frac{1}{2}} + \bar{r}^{n+\frac{1}{2}}(f(\bar{\phi}^{n+\frac{1}{2}}) - s\bar{\phi}^{n+\frac{1}{2}}), \quad (62)$$

$$\frac{r^{n+1} - r^n}{\Delta t} = \alpha \left(-\frac{E_0(\phi^{n+1}) - E_0(\phi^n)}{\Delta t} + \bar{r}^{n+\frac{1}{2}} \int_{\Omega} (f(\bar{\phi}^{n+\frac{1}{2}}) - s\bar{\phi}^{n+\frac{1}{2}}) \frac{\phi^{n+1} - \phi^n}{\Delta t} d\Omega \right). \quad (63)$$

where $\phi^{n+\frac{1}{2}} = \frac{1}{2}(\phi^{n+1} + \phi^n)$, $\bar{\phi}^{n+\frac{1}{2}} = (\frac{3}{2}\phi^n - \frac{1}{2}\phi^{n-1})$, $\bar{r}^{n+\frac{1}{2}} = (\frac{3}{2}r^n - \frac{1}{2}r^{n-1})$.

Theorem 3. The second-order Crank-Nicolson (CN) scheme (61)-(63) for the equivalent system (37)-(39) is unconditionally energy stable in the sense that

$$E_{CM}^{n+1} - E_{CM}^n = -\Delta t \int_{\Omega} \mu^{n+\frac{1}{2}} \mathcal{G}\mu^{n+\frac{1}{2}} d\Omega \leq 0, \quad (64)$$

where the modified discrete version of the energy is defined by

$$E_{CM}^n = \frac{1}{2} \int_{\Omega} \phi^n \mathcal{L}\phi^n d\Omega + \frac{1}{\alpha} r^n + \int_{\Omega} F(\phi^n) d\Omega \quad (65)$$

Proof : We take the L^2 inner product of (61) with $\Delta t \mu^{n+\frac{1}{2}}$ to obtain

$$\int_{\Omega} (\phi^{n+1} - \phi^n) \mu^{n+\frac{1}{2}} d\Omega = -\Delta t \int_{\Omega} \mu^{n+\frac{1}{2}} \mathcal{G}\mu^{n+\frac{1}{2}} d\Omega. \quad (66)$$

By taking the L^2 inner product of (62) with $(\phi^{n+1} - \phi^n)$, we obtain

$$\begin{aligned} & \int_{\Omega} (\phi^{n+1} - \phi^n) \mu^{n+\frac{1}{2}} d\Omega = \frac{1}{2} \int_{\Omega} (\phi^{n+1} \mathcal{L}\phi^{n+1} - \phi^n \mathcal{L}\phi^n) d\Omega \\ & + \frac{s}{2} \left(\int_{\Omega} |\phi^{n+1}|^2 - |\phi^n|^2 \right) d\Omega + \bar{r}^{n+\frac{1}{2}} \int_{\Omega} (f(\bar{\phi}^{n+\frac{1}{2}}) - s\bar{\phi}^{n+\frac{1}{2}}) (\phi^{n+1} - \phi^n) d\Omega \end{aligned} \quad (67)$$

By combining (66) and (67), we can get

$$\begin{aligned} & \frac{1}{2} \int_{\Omega} (\phi^{n+1} \mathcal{L}\phi^{n+1} - \phi^n \mathcal{L}\phi^n) d\Omega + \frac{s}{2} \left(\int_{\Omega} |\phi^{n+1}|^2 - |\phi^n|^2 \right) d\Omega \\ & + \bar{r}^{n+\frac{1}{2}} \int_{\Omega} (f(\bar{\phi}^{n+\frac{1}{2}}) - s\bar{\phi}^{n+\frac{1}{2}})(\phi^{n+1} - \phi^n) d\Omega = -\Delta t \int_{\Omega} \mu^{n+\frac{1}{2}} \mathcal{G}\mu^{n+\frac{1}{2}} d\Omega. \end{aligned} \quad (68)$$

By multiplying (63) with $\frac{\Delta t}{\alpha}$, we obtain

$$\frac{1}{\alpha} (r^{n+1} - r^n) + (E_0(\phi^{n+1}) - E_0(\phi^n)) = \bar{r}^{n+\frac{1}{2}} \int_{\Omega} (f(\bar{\phi}^{n+\frac{1}{2}}) - s\bar{\phi}^{n+\frac{1}{2}})(\phi^{n+1} - \phi^n) d\Omega \quad (69)$$

By combining (68) and (69)

$$\begin{aligned} & \frac{1}{2} \int_{\Omega} (\phi^{n+1} \mathcal{L}\phi^{n+1} - \phi^n \mathcal{L}\phi^n) d\Omega + \frac{s}{2} \left(\int_{\Omega} |\phi^{n+1}|^2 - |\phi^n|^2 \right) d\Omega + \frac{1}{\alpha} (r^{n+1} - r^n) \\ & + (E_0(\phi^{n+1}) - E_0(\phi^n)) = -\Delta t \int_{\Omega} \mu^{n+\frac{1}{2}} \mathcal{G}\mu^{n+\frac{1}{2}} d\Omega. \end{aligned} \quad (70)$$

Using the definition of $E_0(\phi^{n+1})$, $E_0(\phi^{n+1}) = \int_{\Omega} (F(\phi^{n+1}) - \frac{s}{2} |\phi^{n+1}|^2) d\Omega$, we can get

$$\begin{aligned} & \frac{1}{2} \int_{\Omega} (\phi^{n+1} \mathcal{L}\phi^{n+1} - \phi^n \mathcal{L}\phi^n) d\Omega + \frac{1}{\alpha} r^{n+1} - \frac{1}{\alpha} r^n + \int_{\Omega} F(\phi^{n+1}) d\Omega - \int_{\Omega} F(\phi^n) d\Omega \\ & = -\Delta t \int_{\Omega} \mu^{n+\frac{1}{2}} \mathcal{G}\mu^{n+\frac{1}{2}} d\Omega. \end{aligned} \quad (71)$$

3.4. The second-order BDF2 Scheme

The second order BDF2 scheme is given as

$$\frac{3\phi^{n+1} - 4\phi^n + \phi^{n-1}}{2\Delta t} = -\mathcal{G}\mu^{n+1}, \quad (72)$$

$$\mu^{n+1} = \mathcal{L}\phi^{n+1} + s\phi^{n+1} + \bar{r}^{n+\frac{1}{2}} (f(\bar{\phi}^{n+\frac{1}{2}}) - s\bar{\phi}^{n+\frac{1}{2}}), \quad (73)$$

$$\begin{aligned} \frac{3r^{n+1} - 4r^n + r^{n-1}}{2\Delta t} &= \alpha \left(-\frac{3E_0(\phi^{n+1}) - 4E_0(\phi^n) + E_0(\phi^{n-1})}{2\Delta t} \right. \\ & \left. + \bar{r}^{n+\frac{1}{2}} \int_{\Omega} (f(\bar{\phi}^{n+\frac{1}{2}}) - s\bar{\phi}^{n+\frac{1}{2}}) \frac{3\phi^{n+1} - 4\phi^n + \phi^{n-1}}{2\Delta t} d\Omega \right). \end{aligned} \quad (74)$$

where $\bar{\phi}^{n+\frac{1}{2}} = (\frac{3}{2}\phi^n - \frac{1}{2}\phi^{n-1})$, $\bar{r}^{n+\frac{1}{2}} = (\frac{3}{2}r^n - \frac{1}{2}r^{n-1})$.

Theorem 4. The second-order BDF2 scheme (72)-(74) for the equivalent system (37)-(39) is unconditionally energy stable in the sense that

$$E_{CM}^{n+1} - E_{CM}^n \leq -\Delta t \int_{\Omega} \mu^{n+\frac{1}{2}} \mathcal{G}\mu^{n+\frac{1}{2}} d\Omega \leq 0, \quad (75)$$

where the modified discrete version of the energy is defined by

$$\begin{aligned} E_{CM}^n &= \frac{1}{4} \int_{\Omega} (\phi^n \mathcal{L}\phi^n + (2\phi^n - \phi^{n-1}) \mathcal{L}(2\phi^n - \phi^{n-1})) d\Omega \\ & + \frac{s}{4} \int_{\Omega} (|\phi^n|^2 + |2\phi^n - \phi^{n-1}|^2) d\Omega + \frac{1}{2\alpha} (3r^n - r^{n-1}) + \frac{1}{2} (3E_0(\phi^n) - E_0(\phi^{n-1})) \end{aligned} \quad (76)$$

Proof : We take the L^2 inner product of (72) with $\Delta t \mu^{n+1}$ to obtain

$$\frac{1}{2} \int_{\Omega} (3\phi^{n+1} - 4\phi^n + \phi^{n-1}) \mu^{n+1} d\Omega = -\Delta t \int_{\Omega} \mu^{n+1} \mathcal{G} \mu^{n+1} d\Omega. \quad (77)$$

By taking the L^2 inner product of (73) with $\frac{1}{2}(3\phi^{n+1} - 4\phi^n + \phi^{n-1})$, and using the following identity

$$2(3a - 4b + c)a = a^2 + (2a - b)^2 - b^2 - (2b - c)^2 + (a - 2b + c)^2, \quad (78)$$

we obtain

$$\begin{aligned} \frac{1}{2} \int_{\Omega} (3\phi^{n+1} - 4\phi^n + \phi^{n-1}) \mu^{n+1} d\Omega &= \frac{\bar{r}^{n+\frac{1}{2}}}{2} \int_{\Omega} (f(\bar{\phi}^{n+\frac{1}{2}}) - s\bar{\phi}^{n+\frac{1}{2}}) (3\phi^{n+1} - 4\phi^n + \phi^{n-1}) d\Omega \\ \frac{1}{4} \int_{\Omega} (\phi^{n+1} \mathcal{L} \phi^{n+1} + (2\phi^{n+1} - \phi^n) \mathcal{L} (2\phi^{n+1} - \phi^n) - \phi^n \mathcal{L} \phi^n - (2\phi^n - \phi^{n-1}) \mathcal{L} (2\phi^n - \phi^{n-1}) \\ &+ (\phi^{n+1} - 2\phi^n + \phi^{n-1}) \mathcal{L} (\phi^{n+1} - 2\phi^n + \phi^{n-1})) d\Omega \\ &+ \frac{s}{4} \int_{\Omega} (|\phi^{n+1}|^2 + |2\phi^{n+1} - \phi^n|^2 - |\phi^n|^2 - |2\phi^n - \phi^{n-1}|^2 + |\phi^{n+1} - 2\phi^n + \phi^{n-1}|^2) d\Omega. \end{aligned} \quad (79)$$

By combining (77) and (79), we can get

$$\begin{aligned} \frac{1}{4} \int_{\Omega} (\phi^{n+1} \mathcal{L} \phi^{n+1} + (2\phi^{n+1} - \phi^n) \mathcal{L} (2\phi^{n+1} - \phi^n) - \phi^n \mathcal{L} \phi^n - (2\phi^n - \phi^{n-1}) \mathcal{L} (2\phi^n - \phi^{n-1}) \\ &+ (\phi^{n+1} - 2\phi^n + \phi^{n-1}) \mathcal{L} (\phi^{n+1} - 2\phi^n + \phi^{n-1})) d\Omega \\ &+ \frac{s}{4} \int_{\Omega} (|\phi^{n+1}|^2 + |2\phi^{n+1} - \phi^n|^2 - |\phi^n|^2 - |2\phi^n - \phi^{n-1}|^2 + |\phi^{n+1} - 2\phi^n + \phi^{n-1}|^2) d\Omega \\ &+ \frac{\bar{r}^{n+\frac{1}{2}}}{2} \int_{\Omega} (f(\bar{\phi}^{n+\frac{1}{2}}) - s\bar{\phi}^{n+\frac{1}{2}}) (3\phi^{n+1} - 4\phi^n + \phi^{n-1}) d\Omega = -\Delta t \int_{\Omega} \mu^{n+1} \mathcal{G} \mu^{n+1} d\Omega. \end{aligned} \quad (80)$$

By multiplying (74) with $\frac{\Delta t}{\alpha}$, we obtain

$$\begin{aligned} \frac{1}{2\alpha} (3r^{n+1} - 4r^n + r^{n-1}) + \frac{1}{2} (3E_0(\phi^{n+1}) - 4E_0(\phi^n) + E_0(\phi^{n-1})) = \\ \frac{\bar{r}^{n+\frac{1}{2}}}{2} \int_{\Omega} (f(\bar{\phi}^{n+\frac{1}{2}}) - s\bar{\phi}^{n+\frac{1}{2}}) (3\phi^{n+1} - 4\phi^n + \phi^{n-1}) d\Omega. \end{aligned} \quad (81)$$

By combining (80) and (81)

$$\begin{aligned} \frac{1}{4} \int_{\Omega} (\phi^{n+1} \mathcal{L} \phi^{n+1} + (2\phi^{n+1} - \phi^n) \mathcal{L} (2\phi^{n+1} - \phi^n) - \phi^n \mathcal{L} \phi^n - (2\phi^n - \phi^{n-1}) \mathcal{L} (2\phi^n - \phi^{n-1}) \\ &+ (\phi^{n+1} - 2\phi^n + \phi^{n-1}) \mathcal{L} (\phi^{n+1} - 2\phi^n + \phi^{n-1})) d\Omega \\ &+ \frac{s}{4} \int_{\Omega} (|\phi^{n+1}|^2 + |2\phi^{n+1} - \phi^n|^2 - |\phi^n|^2 - |2\phi^n - \phi^{n-1}|^2 + |\phi^{n+1} - 2\phi^n + \phi^{n-1}|^2) d\Omega \\ &+ \frac{1}{2\alpha} (3r^{n+1} - 4r^n + r^{n-1}) - \frac{1}{2\alpha} (3r^n - r^{n-1}) + \frac{1}{2} (3E_0(\phi^{n+1}) - E_0(\phi^n)) - \frac{1}{2} (3E_0(\phi^n) - E_0(\phi^{n-1})) \\ &= -\Delta t \int_{\Omega} \mu^{n+1} \mathcal{G} \mu^{n+1} d\Omega. \end{aligned} \quad (82)$$

Taking the first-order numerical scheme of the Allen-Cahn equation as an example, we aim to demonstrate that by making certain assumptions about the numerical solutions, as the parameter α and Δt decreases, the solution of equation (50)-(52) converges to the solution of equation (8)-(9), and $\frac{r^n}{\alpha}$ converges to $\frac{1}{\alpha}$, which means the difference between the discrete energy (76) and the original energy is a constant.

The first-order numerical scheme of Allen-Cahn equation:

$$\frac{\phi^{n+1} - \phi^n}{\Delta t} = -\mu^{n+1}, \quad (83)$$

$$\mu^{n+1} = -\Delta\phi^{n+1} + s\phi^{n+1} + r^n g(\phi^n), \quad (84)$$

$$\frac{r^{n+1} - r^n}{\Delta t} = \alpha \left(-\frac{E_0(\phi^{n+1}) - E_0(\phi^n)}{\Delta t} + r^n \int_{\Omega} g(\phi^n) \frac{\phi^{n+1} - \phi^n}{\Delta t} d\Omega \right), \quad (85)$$

where $g(\phi^n) = f(\phi^n) - s\phi^n$.

The Original Allen-Cahn system:

$$\phi_t = -\mu, \quad (86)$$

$$\mu = -\Delta\phi + f(\phi), \quad (87)$$

Theorem 5. Assume that $\phi(t_0) \in \mathbf{H}^2(\Omega)$, $\phi^n \in \mathbf{H}^2(\Omega)$, $\phi_t \in \mathbf{L}^\infty(0, T; \mathbf{L}^2(\Omega))$, $\phi_{tt} \in \mathbf{L}^2(0, T; \mathbf{L}^2(\Omega))$, We then have

(i). $\lim_{\alpha \rightarrow 0} |r^n - 1| = 0$.

(ii). $\lim_{\Delta t \rightarrow 0} \frac{1}{\alpha} |r^n - 1| = 0$.

(iii). For all $n \leq T/\Delta t$, $\exists \alpha_0$, $\forall \alpha \leq \alpha_0$, we have

$$\frac{1}{2} \|\nabla e^n\|^2 + \frac{s}{2} \|e^n\|^2 \leq C \exp((1 - C\Delta t)^{-1} C t^n) \left(\Delta t^2 \int_0^{t_n} \|\phi_{tt}(s)\|^2 + \|\phi_t(s)\|^2 ds + \Delta t \alpha \right). \quad (88)$$

The constant C is dependent on T , $\phi(t_0)$, $|\Omega|$, $\|\phi\|_{\mathbf{L}^\infty(0, T; W^{1, \infty}(\Omega))}$, $\|\phi_t\|_{\mathbf{L}^\infty(0, T; \mathbf{L}^2(\Omega))}$.

Proof: see the Appendix.

4. The CSAV approach for gradient flows of several functions

In certain cases, the nonlinear part of the free energy may consist of various terms. When using a single SAV method, small time steps are often required to obtain accurate solutions [30]. However, it has been demonstrated in [30] that the multiple SAV (MSAV) approach can overcome this limitation. Extending the CSAV method to include more than two distinct nonlinear terms can be easily implemented.

$$\begin{cases} \frac{\partial \phi}{\partial t} = -\mathcal{G}\mu \\ \mu = \mathcal{L}\phi + F_1'(\phi) + F_2'(\phi) \end{cases} \quad (89)$$

where \mathcal{L} is a linear self-adjoint elliptic operator, $F_1(\phi), F_2(\phi)$ are nonlinear potential function, \mathcal{G} is a semi-positive definite linear operator. The system (89) satisfies an energy dissipation law as follows:

$$\frac{dE_{multi}(\phi)}{dt} = -(\mathcal{G}\mu, \mu)$$

where

$$E_{multi}(\phi) = \frac{1}{2}(\mathcal{L}\phi, \phi) + \int_{\Omega} F_1(\phi)d\mathbf{x} + \int_{\Omega} F_2(\phi)d\mathbf{x}.$$

We define $E_i = \int_{\Omega} (F_i(\phi) - \frac{1}{2}s_i\phi^2) d\Omega$, $i = 1, 2$, and introduce the following constant scalar auxiliary variables:

$$\begin{cases} \frac{dr_i}{dt} = \alpha \left(-\frac{dE_i}{dt} + r_i \int_{\Omega} F_i'(\phi)\phi_t d\Omega \right), \quad i = 1, 2 \\ r_i(t)|_{t=0} = 1, \quad i = 1, 2. \end{cases} \quad (90)$$

Then, we can rewrite the equation (89) as

$$\begin{cases} \frac{\partial \phi}{\partial t} = -\mathcal{G}\mu, \\ \mu = \frac{\delta E}{\delta \phi} = \mathcal{L}\phi + (s_1 + s_2)\phi + r_1 F_1'(\phi) + r_2 F_2'(\phi), \\ \frac{dr_1}{dt} = \alpha \left(-\frac{dE_1}{dt} + r_1 \int_{\Omega} F_1'(\phi)\phi_t d\Omega \right), \\ \frac{dr_2}{dt} = \alpha \left(-\frac{dE_2}{dt} + r_2 \int_{\Omega} F_2'(\phi)\phi_t d\Omega \right) \end{cases} \quad (91)$$

Taking the inner products of the first two equations above with μ , ϕ_t , respectively, and summing up the third and fourth equation, we obtain that the above equivalent system satisfies a modified energy dissipation law:

$$\frac{d}{dt} \left[\frac{1}{2}(\phi, \mathcal{L}\phi) + E_1 + E_2 + \frac{r_1}{\alpha} + \frac{r_2}{\alpha} \right] = -(\mathcal{G}\mu, \mu) \leq 0 \quad (92)$$

The first-order scheme can be derived using the backward Euler method, and the second-order scheme can be obtained by applying the Crank-Nicolson formula. Specifically, the first-order scheme is given by:

$$\frac{\phi^{n+1} - \phi^n}{\Delta t} = -\mathcal{G}\mu^{n+1}, \quad (93)$$

$$\mu^{n+1} = \mathcal{L}\phi^{n+1} + (s_1 + s_2)\phi^{n+1} + r_1^n F_1'(\phi^n) + r_2^n F_2'(\phi^n), \quad (94)$$

$$\frac{r_1^{n+1} - r_1^n}{\Delta t} = \alpha \left(-\frac{E_1(\phi^{n+1}) - E_1(\phi^n)}{\Delta t} + r_1^n \int_{\Omega} F_1'(\phi^n) \frac{\phi^{n+1} - \phi^n}{\Delta t} d\Omega \right). \quad (95)$$

$$\frac{r_2^{n+1} - r_2^n}{\Delta t} = \alpha \left(-\frac{E_2(\phi^{n+1}) - E_2(\phi^n)}{\Delta t} + r_2^n \int_{\Omega} F_2'(\phi^n) \frac{\phi^{n+1} - \phi^n}{\Delta t} d\Omega \right). \quad (96)$$

and the second-order scheme is

$$\frac{\phi^{n+1} - \phi^n}{\Delta t} = -\mathcal{G}\mu^{n+\frac{1}{2}}, \quad (97)$$

$$\mu^{n+\frac{1}{2}} = \mathcal{L}\phi^{n+\frac{1}{2}} + (s_1 + s_2)\phi^{n+\frac{1}{2}} + \bar{r}_1^{n+\frac{1}{2}}F_1'(\bar{\phi}^{n+\frac{1}{2}}) + \bar{r}_2^{n+\frac{1}{2}}F_2'(\bar{\phi}^{n+\frac{1}{2}}), \quad (98)$$

$$\frac{r_1^{n+1} - r_1^n}{\Delta t} = \alpha \left(-\frac{E_1(\phi^{n+1}) - E_1(\phi^n)}{\Delta t} + \bar{r}_1^{n+\frac{1}{2}} \int_{\Omega} F_1'(\bar{\phi}^{n+\frac{1}{2}}) \frac{\phi^{n+1} - \phi^n}{\Delta t} d\Omega \right). \quad (99)$$

$$\frac{r_2^{n+1} - r_2^n}{\Delta t} = \alpha \left(-\frac{E_2(\phi^{n+1}) - E_2(\phi^n)}{\Delta t} + \bar{r}_2^{n+\frac{1}{2}} \int_{\Omega} F_2'(\bar{\phi}^{n+\frac{1}{2}}) \frac{\phi^{n+1} - \phi^n}{\Delta t} d\Omega \right). \quad (100)$$

where $\phi^{n+\frac{1}{2}} = \frac{1}{2}(\phi^{n+1} + \phi^n)$, $\bar{\phi}^{n+\frac{1}{2}} = (\frac{3}{2}\phi^n - \frac{1}{2}\phi^{n-1})$, $\bar{r}_i^{n+\frac{1}{2}} = (\frac{3}{2}r_i^n - \frac{1}{2}r_i^{n-1})$.

Similar to the proof of **Theorem 2** and **Theorem 3**, we can prove the unconditional energy stability of the above two schemes.

Theorem 6. The first-order scheme (93)-(96) for the equivalent system (91) is unconditionally energy stable in the sense that

$$E_{multi}^{n+1} - E_{multi}^n \leq -\Delta t \int_{\Omega} \mu^{n+1} \mathcal{G}\mu^{n+1} d\Omega. \quad (101)$$

where the modified discrete version of the energy is defined by

$$E_{multi}^n = \frac{1}{2} \int_{\Omega} \phi^{n+1} \mathcal{L}\phi^{n+1} d\Omega + \frac{1}{\alpha} r_1^{n+1} + \frac{1}{\alpha} r_2^{n+1} + \int_{\Omega} F_1(\phi^{n+1}) d\Omega + \int_{\Omega} F_2(\phi^{n+1}) d\Omega \quad (102)$$

Theorem 7. The second-order Crank-Nicolson (CN) scheme (97)-(100) for the equivalent system (91) is unconditionally energy stable in the sense that

$$E_{multi}^{n+1} - E_{multi}^n \leq -\Delta t \int_{\Omega} \mu^{n+\frac{1}{2}} \mathcal{G}\mu^{n+\frac{1}{2}} d\Omega. \quad (103)$$

where the modified discrete version of the energy is defined by

$$E_{multi}^n = \frac{1}{2} \int_{\Omega} \phi^{n+1} \mathcal{L}\phi^{n+1} d\Omega + \frac{1}{\alpha} r_1^{n+1} + \frac{1}{\alpha} r_2^{n+1} + \int_{\Omega} F_1(\phi^{n+1}) d\Omega + \int_{\Omega} F_2(\phi^{n+1}) d\Omega \quad (104)$$

5. Numerical results

In this section, we implement the proposed numerical methods and apply them to various classical phase-field models, including the Allen-Cahn (AC) equation, the Cahn-Hilliard (CH) equation, the Molecular Beam Epitaxy (MBE) model, the phase-field crystal (PFC) model, and the diblock copolymer model.

For this study, we consider phase-field models with periodic boundary conditions. The Finite Element Method (FEM) is employed for spatial discretization. The spatial domain $\Omega = [0, L_x] \times [0, L_y]$ is divided into a uniform grid with a mesh size of $h_x = L_x/N_x$ and $h_y = L_y/N_y$, where N_x and N_y are positive even integers. Unless otherwise

stated, we set $N_x = N_y = 128$ for all cases. Since both the BDF2 and CN schemes offer second-order accuracy, our focus in this paper is on comparing the original SAV-CN scheme with the RSAV-CN scheme and the CSAV-CN scheme.

The accurate energy mentioned in the following numerical examples is obtained from the results of the second-order CN scheme (61)-(63) with $\alpha = 0$ and $\Delta t = 10^{-5}$, which degrades to the semi-implicit/CN numerical scheme. The CSAV modified energy is equal to E_{CM} in equation (41) after subtracting a constant $\frac{r}{\alpha}$, as mentioned in equation (49). The RSAV modified energy and the SAV modified energy are E_M in equation (14).

5.1. Allen-Cahn and Cahn-Hilliard equations

Consider the free energy $E(\phi) = \int_{\Omega} \frac{\epsilon^2}{2} |\nabla \phi|^2 + \frac{1}{4} (\phi^2 - 1)^2 d\Omega$, with mobility operator $\mathcal{G} = 1$, the general gradient flow model in (4)-(5) reduces to the corresponding Allen-Cahn (AC) equation.

$$\phi_t = -\lambda(-\epsilon^2 \Delta \phi + \phi^3 - \phi). \quad (105)$$

If the mobility operator is $\mathcal{G} = \lambda \Delta$, the gradient flow model in (4)-(5) reduces to the Cahn-Hilliard (CH) equation.

$$\phi_t = \Delta \mu, \quad (106)$$

$$\mu = \lambda(-\epsilon^2 \Delta \phi + \phi^3 - \phi), \quad (107)$$

Example 1. We first verify that the CSAV-CN scheme is second-order accurate in time. For the Allen-Cahn equation, consider the domain $\Omega = [0, 2\pi]^2$, and we choose the smooth initial condition

$$\phi_0(x, y, 0) = \sum_{i=1}^2 \tanh \left(\frac{\sqrt{(x - x_i)^2 + (y - y_i)^2} - R_i}{\sqrt{2}\epsilon} \right) + 1, \quad (108)$$

where $R_1 = 1.4$, $R_2 = 0.5$, $(x_1, y_1) = (\pi - 0.8, \pi)$, and $(x_2, y_2) = (\pi + 1.7, \pi)$. To solve the AC equation, we use uniform meshes $N_x = N_y = 128$ and set the model parameters: $\epsilon = 0.08$ and $\lambda = 1$, the numerical parameters: $s = 4$. We choose three different $\alpha = 1, 0.1, 0.0001$. Since the analytical solutions are unknown, we consider the numerical solutions obtained with a smaller time step size and smaller α , namely $\Delta t = 3.125 \times 10^{-4}$ and $\alpha = 1 \times 10^{-5}$, as an approximation of the exact solution. The numerical errors of ϕ in L^2 norm with different time steps and different α at $t = 0.5$ are summarized in Table 1, and the numerical errors of r are summarized in the Fig.1(a). We observe second-order convergence for both the numerical solutions of ϕ and r , and the accuracy of ϕ and r increases as the value of α decreases, which also verifies the conclusion of **Theorem 5**.

For the Cahn-Hilliard equation, we use the same initial condition (108). The model parameters are set as $\epsilon = 0.08$ and $\lambda = 0.125$. We solve the CH equation using uniform meshes $N_x = N_y = 256$, with numerical parameters $s = 4$ and $\alpha = 1, 0.1, 0.01$. Since the analytical solutions are unknown, we consider the numerical solutions obtained with a

| Δt | $\ e(\phi)\ _{L^2} (\alpha = 1)$ | Order | $\ e(\phi)\ _{L^2} (\alpha = 0.1)$ | Order | $\ e(\phi)\ _{L^2} (\alpha = 0.0001)$ | Order |
|-----------------------|----------------------------------|-------|------------------------------------|-------|---------------------------------------|-------|
| 6.25×10^{-4} | 2.17×10^{-9} | | 2.149×10^{-9} | | 2.148×10^{-9} | |
| 1.25×10^{-3} | 1.08×10^{-8} | 2.31 | 1.075×10^{-8} | 2.32 | 1.074×10^{-8} | 2.32 |
| 2.5×10^{-3} | 4.54×10^{-8} | 2.07 | 4.513×10^{-8} | 2.06 | 4.511×10^{-8} | 2.07 |
| 5×10^{-3} | 1.84×10^{-7} | 2.01 | 1.827×10^{-7} | 2.02 | 1.826×10^{-7} | 2.02 |
| 1×10^{-2} | 7.37×10^{-7} | 2.00 | 7.327×10^{-7} | 2.00 | 7.324×10^{-7} | 2.00 |
| 2×10^{-2} | 2.95×10^{-6} | 2.00 | 2.932×10^{-6} | 2.00 | 2.931×10^{-6} | 2.00 |

Table 1: Convergence tests where the L^2 numerical errors of the phase-field variable ϕ at $t=0.5$ for different $\alpha = 1, 0.1, 0.0001$ in the Allen-Cahn equation.

smaller time step size and smaller α , namely $\delta t = 7.8125 \times 10^{-5}$ and $\alpha = 1 \times 10^{-5}$, as an approximation of the exact solution. The numerical errors of ϕ in L^2 norm with different time steps at $t = 0.125$ are summarized in Table 2, and the numerical errors of r are summarized in the Fig.1(b). We observe second-order convergence for both the numerical solutions of ϕ and r , and the accuracy of ϕ and r increases as the value of α decreases.

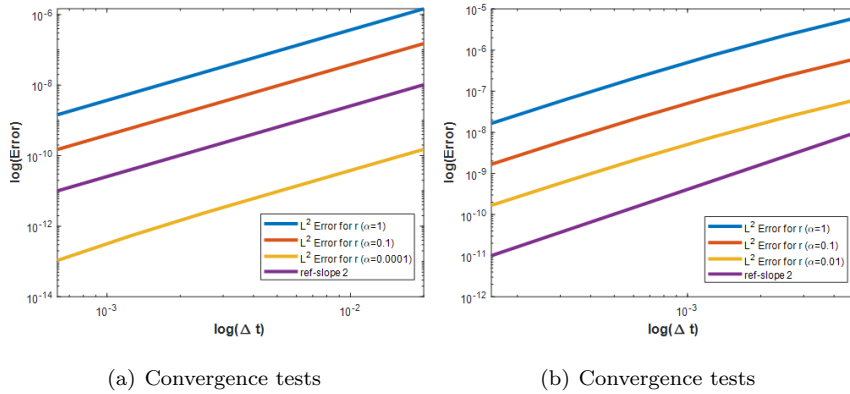


Figure 1: (a) Convergence tests of the auxiliary variable r at $t=0.5$ for different α in the Allen-Cahn equation. (b) Convergence tests of the auxiliary variable r at $t=0.121$ for different α in the Cahn-Hilliard equation.

Example 2. In this example, we perform the energy stability tests and investigate the impact of different α on the numerical results. Taking the Cahn-Hilliard equation as an example, we consider the domain $\Omega = [0, 2\pi]^2$, and use the same initial condition as the CH case in (108). We set the model parameters $\epsilon = 0.08$ and $\lambda = 1$ and numerical parameters $s = 4$. In Fig. 2(a), we set $\alpha = 10^{-3}$ and plot the time evolution of the energy functional for the different time step sizes $\Delta t = 2 \times 10^{-2}, 1 \times 10^{-2}, 1 \times 10^{-3}$. We observe that all energy curves show the monotonic decay for all time steps, confirming the unconditional energy stability of the CSAV scheme. In Fig. 2(b),

| Δt | $\ e(\phi)\ _{L^2} (\alpha = 1)$ | Order | $\ e(\phi)\ _{L^2} (\alpha = 0.1)$ | Order | $\ e(\phi)\ _{L^2} (\alpha = 0.01)$ | Order |
|-------------------------|----------------------------------|-------|------------------------------------|-------|-------------------------------------|-------|
| 1.5625×10^{-4} | 1.09×10^{-8} | | 5.43×10^{-9} | | 5.03×10^{-9} | |
| 3.125×10^{-4} | 4.60×10^{-8} | 2.07 | 2.66×10^{-8} | 2.29 | 2.51×10^{-8} | 2.32 |
| 6.25×10^{-4} | 1.78×10^{-7} | 1.95 | 1.11×10^{-7} | 2.06 | 1.06×10^{-7} | 2.08 |
| 1.25×10^{-3} | 6.65×10^{-7} | 1.90 | 4.46×10^{-7} | 2.01 | 4.29×10^{-7} | 2.02 |
| 2.5×10^{-3} | 2.43×10^{-6} | 1.87 | 1.78×10^{-6} | 2.00 | 1.73×10^{-6} | 2.01 |
| 5×10^{-3} | 8.88×10^{-6} | 1.87 | 7.18×10^{-6} | 2.01 | 7.03×10^{-6} | 2.02 |

Table 2: Convergence tests where the L^2 numerical errors of the phase-field variable ϕ at $t=0.125$ for different $\alpha = 1, 0.1, 0.01$ in the Cahn-Hilliard equation.

we set $\Delta t = 1 \times 10^{-2}$ and plot the time evolution of the energy functional $E_{CM} - \frac{1}{\alpha}$ for different values of α : $\alpha = 1$ and 1×10^{-3} . We observe that the value of α does not affect energy dissipation, and as α decreases, the system's energy approaches the accurate energy. In Fig. 3(a), we show the evolution of r_n for different α , $\alpha = 1, 1 \times 10^{-3}$. In Figure 3(b), we illustrate the evolution of ϕ over time. As time evolves, the fluid within smaller bubbles dissolves into the surrounding fluid and diffuses towards larger bubbles, causing them to grow. This observation agrees with the phenomenon of Ostwald ripening in an open system. The accurate simulation demonstrates the effectiveness of our CSAV approach.

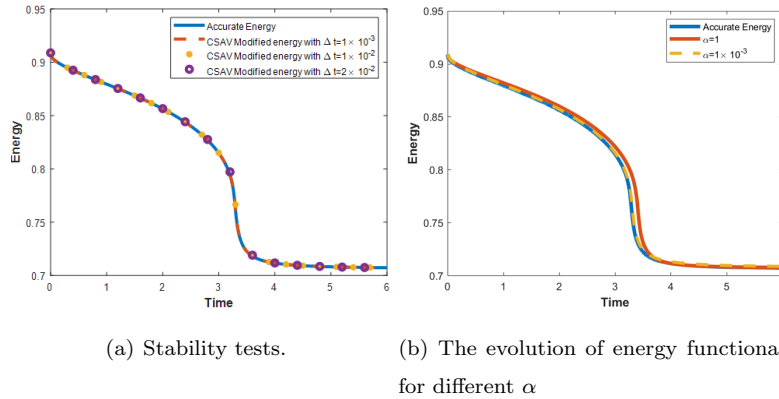


Figure 2: (a) The time evolution of the energy functional for the different time step sizes $\Delta t = 2 \times 10^{-2}, 1 \times 10^{-2}, 1 \times 10^{-3}$ in Example 2. (b) The time evolution of the energy functional for the different α in Example 2.

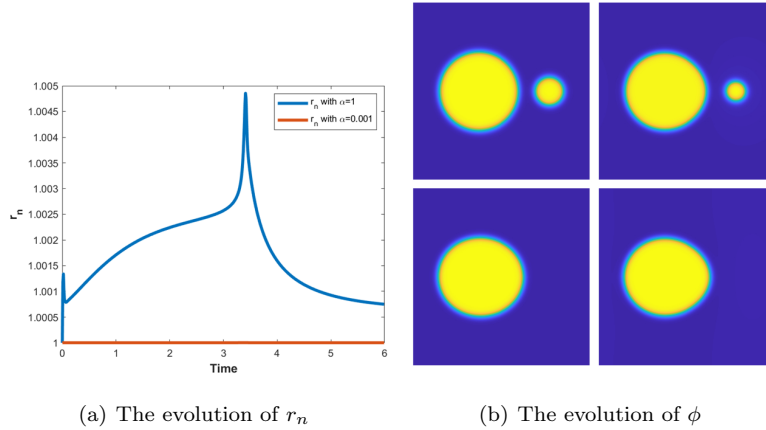


Figure 3: (a) The evolution of r_n for different α in Example 2. (b) Snapshots of the phase variable ϕ are taken at $t=0, 2, 4, 6$ in clockwise sense in Example 2.

Example 3. We now compare our CSAV-CN scheme with the original SAV-CN scheme by solving a benchmark problem for the Allen-Cahn equation. This benchmark problem is widely used in articles such as [20]. The parameter values we use are: $\epsilon = 0.01$, $\lambda = 0.01$, $\Omega = [0, 1]^2$, and numerical parameters $s = 4$, $\alpha = 10^{-6}$. The initial condition is selected as follows:

$$\phi_0(x, y, 0) = \sum_{i=1}^2 \tanh \left(\frac{\sqrt{(x-x_i)^2 + (y-y_i)^2} - R_0}{\sqrt{2}\epsilon} \right) + 1 \quad (109)$$

with the radius $R_0 = 0.19$, $(x_1, y_1) = (0.3, 0.5)$, and $(x_2, y_2) = (0.7, 0.5)$. Initially, two bubbles, entered at $(0.3, 0.5)$ and $(0.7, 0.5)$, respectively, and they are in contact with each other.

In Fig.4(a), the CSAV method exhibits higher accuracy than the original SAV method, even when using a larger time step. In addition, our previous analysis indicates that the coefficients $\frac{q^{n+\frac{1}{2}}}{\sqrt{E_0(\bar{\phi}^{n+\frac{1}{2}})+C_0}}$ in (19) and $\bar{r}^{n+\frac{1}{2}}$ in (62) must approach 1 for the original system to be equivalent to the modified system. The values of these coefficients are presented in Fig.4(b). We observe that the CSAV method effectively maintains the consistency between the modified system and the original system after temporal discretization. In Fig. 5, we show the evolution of the solution over time, where the two bubbles gradually merge into a single bubble, which subsequently shrinks and eventually disappears. The accurate simulation of this phenomenon confirms the effectiveness of our CSAV approach.

Example 4. In this example, we compare the performance of our CSAV-CN scheme with the original SAV-CN scheme and RSAV-CN scheme. For the Allen-Cahn equation, we consider the domain $\Omega = [0, L_x] \times [0, L_y]$ and choose

the initial condition as follows:

$$\phi(x, y) = \tanh \frac{1.5 + 1.2 \cos(6\theta) - 2\pi r}{\sqrt{2}\epsilon} \quad (110)$$

$$\theta = \arctan \frac{y - 0.5L_y}{x - 0.5L_x}, \quad r = \sqrt{\left(x - \frac{L_x}{2}\right)^2 + \left(y - \frac{L_y}{2}\right)^2}. \quad (111)$$

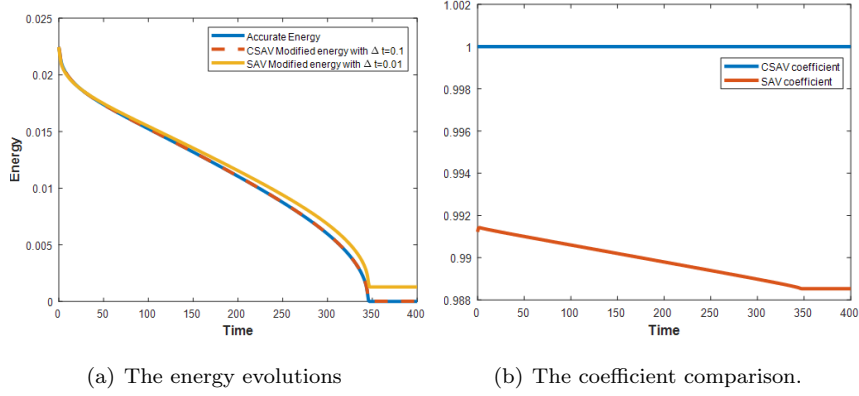


Figure 4: (a) The comparisons of the CSAV modified energy and SAV modified energy in Example 3. (b) The comparisons of the coefficients in (19) and (62) for Example 3.

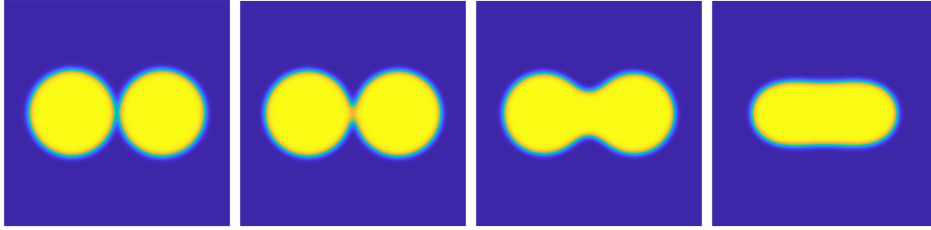


Figure 5: Snapshots of the phase variable ϕ at $t=0, 0.01, 0.1, 1$ for Example 3.

We consider the parameters $L_x = L_y = 1$, $\epsilon = 0.01$, and $\lambda = 1$. Fig. 6(a) demonstrates that the CSAV-CN method achieves higher accuracy compared to the RSAV-CN and SAV-CN methods. In addition, we compare the coefficients $\frac{q^{n+\frac{1}{2}}}{\sqrt{E_0(\bar{\phi}^{n+\frac{1}{2}})+C_0}}$ in (19), $\frac{\bar{q}^{n+\frac{1}{2}}}{\sqrt{E_0(\bar{\phi}^{n+\frac{1}{2}})+C_0}}$ in (22), and $\bar{r}^{n+\frac{1}{2}}$ in (62). Their values are shown in Fig.6(b). We observe that the CSAV method can effectively better preserve the consistency between the modified system and the original system after temporal discretization.

For the Cahn-Hilliard equation, we choose the same initial condition and the computational domain as in the example above. The model parameters used are $\lambda = 0.01$, $\epsilon = 0.01$, and we set the numerical parameters $s = 4$, $\alpha = 10^{-3}$. In Fig.8(a), we display the calculated energy curve for the SAV, RSAV, and CSAV methods. It can be

observed that the energy curve of the CSAV method is closer to the accurate energy compared to SAV and RSAV. This indicates that the CSAV method achieves higher accuracy in dissipating the energy of the system. Furthermore, in Fig.8(b), we compare the coefficients $\frac{q^{n+\frac{1}{2}}}{\sqrt{E_0(\bar{\phi}^{n+\frac{1}{2}})+C_0}}$ in (19), $\frac{\bar{q}^{n+\frac{1}{2}}}{\sqrt{E_0(\bar{\phi}^{n+\frac{1}{2}})+C_0}}$ in (22), and $\bar{r}^{n+\frac{1}{2}}$ in (62). It can be observed that the coefficient of the CSAV method is closer to 1 compared to SAV and RSAV. This indicates a higher numerical consistency between the modified system and the original system for the CSAV method. In Fig.8(c), We compare the energy evolution for $\alpha = 1, 0.001$ when $\Delta t = 5 \times 10^{-3}$ and compare them with the accurate energy computed by using the second-order CN scheme (61)-(63) with $\alpha = 0$ and $\Delta t = 10^{-5}$. We observed that when $\alpha = 0.001$, the energy curve is closer to the accurate energy. This indicates that small α effectively ensures the consistency between the original system and the modified system.

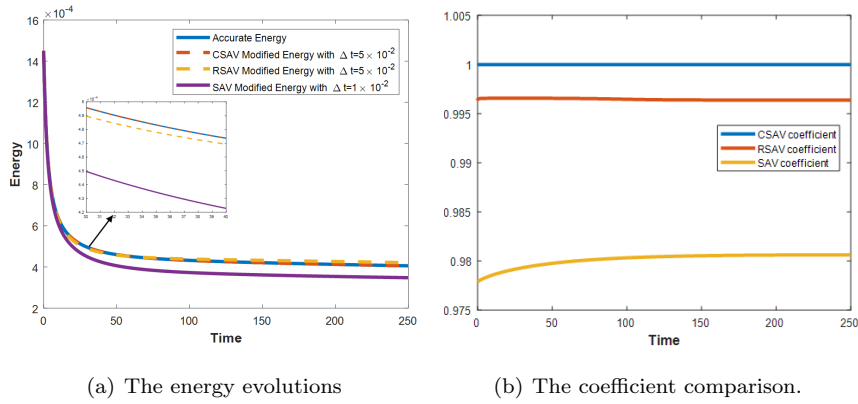


Figure 6: (a) The comparisons of the CSAV modified energy, the RSAV modified energy, the SAV modified energy for the Allen-Cahn equation in Example 4. (b) The comparisons of the coefficients in (19), (22) and (62) for the Allen-Cahn equation in Example 4.

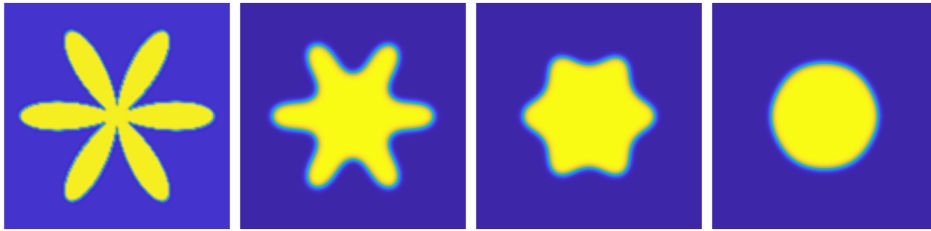


Figure 7: Snapshots of the phase variable ϕ at $t=0, 50, 100, 200$ for Example 4 (Allen-Cahn equation).

5.2. Molecular beam epitaxy model with slope selection

Example 5. In this example, we investigate the molecular beam epitaxy (MBE) model with slope selection. ϕ represents the MBE thickness, and the free energy is defined as $E(\phi) = \int_{\Omega} \left(\frac{\epsilon^2}{2} (\Delta \phi)^2 + \frac{1}{4} (\phi^2 - 1)^2 \right) d\Omega$. The mobility

operator is $\mathcal{G} = 1$. The gradient flow equation is given by:

$$\phi_t = -\epsilon^2 \Delta^2 \phi + \nabla \cdot (|\nabla \phi|^2 - 1) \nabla \phi. \quad (112)$$

The modified system is

$$\partial_t \phi = -\epsilon^2 \Delta^2 \phi + s \Delta \phi + r \nabla \cdot ((|\nabla \phi|^2 - 1 - s) \nabla \phi), \quad (113)$$

$$r_t = \alpha \left(-\frac{dE_{mbe0}}{dt} + r \int_{\Omega} (|\nabla \phi|^2 - 1 - s) \nabla \phi \cdot \nabla \phi_t d\Omega \right), \quad (114)$$

where $E_{mbe0} = \frac{1}{4} \int_{\Omega} (|\nabla \phi|^2 - 1 - s)^2 d\Omega$.

The Second-order CN scheme is the following,

$$\frac{\phi^{n+1} - \phi^n}{\Delta t} = -\epsilon^2 \Delta \phi^{n+\frac{1}{2}} + s \Delta \phi^{n+\frac{1}{2}} + r \nabla \cdot \left((|\nabla \bar{\phi}^{n+\frac{1}{2}}|^2 - 1 - s) \nabla \bar{\phi}^{n+\frac{1}{2}} \right), \quad (115)$$

$$\mu^{n+\frac{1}{2}} = \Delta \phi^{n+\frac{1}{2}}, \quad (116)$$

$$\frac{r^{n+1} - r^n}{\Delta t} = \alpha \left(-\frac{E_{mbe0}^{n+1} - E_{mbe0}^n}{\Delta t} + \bar{r}^{n+\frac{1}{2}} \int_{\Omega} \left((|\nabla \bar{\phi}^{n+\frac{1}{2}}|^2 - 1 - s) \nabla \bar{\phi}^{n+\frac{1}{2}} \right) \cdot \nabla \frac{\phi^{n+1} - \phi^n}{\Delta t} d\Omega \right). \quad (117)$$

We use the classical benchmark problem for the MBE model. Mainly we consider the domain $\Omega = [0, 2\pi]^2$, with $\epsilon^2 = 0.1$. we choose the smooth initial condition

$$\phi(x, y, t = 0) = 0.1(\sin(3x)\sin(2y) + \sin(5x)\sin(5y)), \quad (118)$$

and solve the MBE model with slope selection using $s = 4$ and $\alpha = 10^{-5}$. In Fig.9(a), we present the energy curve obtained with a time step of $\Delta t = 0.001$, which matches closely with the accurate energy. The evolution of r_n is depicted in Fig.9(b). It can be observed that r_n is sufficiently close to 1, indicating a high numerical consistency between the modified and original systems. The solution contours at $t = 0, 1, 6$, and 16 are plotted in Fig.10, which agree with the results reported in [31].

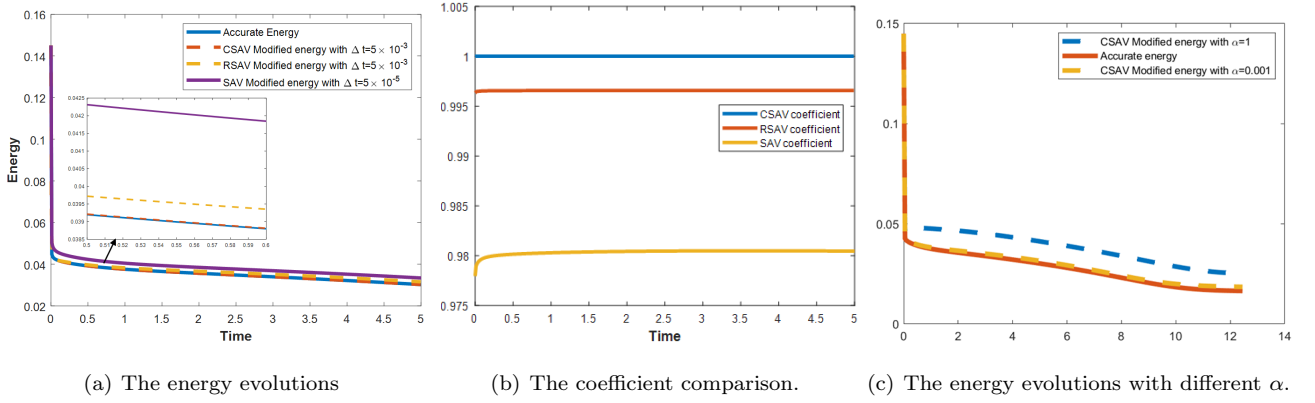


Figure 8: (a) The comparisons of the CSAV modified energy, the RSAV modified energy, the SAV modified energy for the Cahn-Hilliard equation in Example 4. (b) The comparisons of the coefficients in (19), (22) and (62) for the Cahn-Hilliard equation in Example 4. (c) The energy evolutions with different $\alpha = 1, 0.001$ when $\Delta t = 5 \times 10^{-3}$ for the Cahn-Hilliard equation in Example 4.

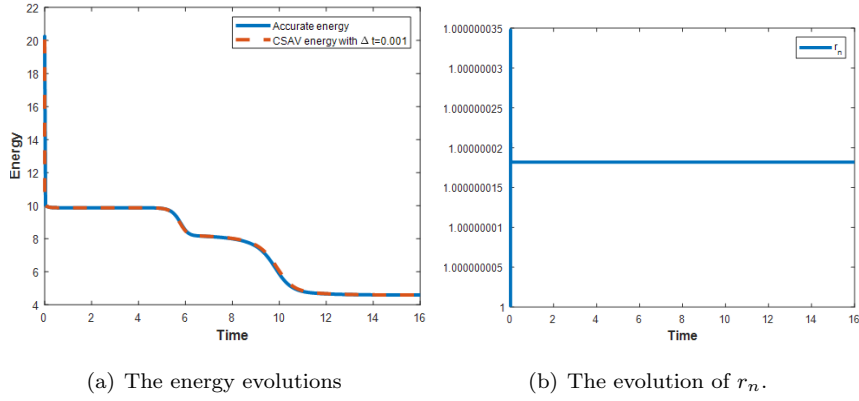


Figure 9: (a) The evolution of energy computed by using the time step $\Delta t = 0.001$ for Example 5. (b) The evolution of r_n for Example 5.

5.3. Applications to other phase-field models

We now apply the CSAV method to other phase field models, including the phase-field crystal model and the diblock copolymer model.

Firstly, we consider its application to the phase field crystal (PFC) model. Consider the free energy $E = \int_{\Omega} \frac{1}{2} \phi (a_0 + \Delta)^2 \phi + \frac{1}{4} \phi^4 - \frac{b_0}{2} \phi^2 d\Omega$, where a_0 and b_0 are model parameters, and the mobility operator is defined as $\mathcal{G} = -\lambda \Delta$. By applying the CSAV method, the general gradient flow model in (4)-(5) can be reduced to the PFC

model, which can be expressed as follows:

$$\partial_t \phi = \lambda \Delta \mu, \quad (119)$$

$$\mu = -(a_0 + \Delta)^2 \phi + \phi^3 - b_0 \phi. \quad (120)$$

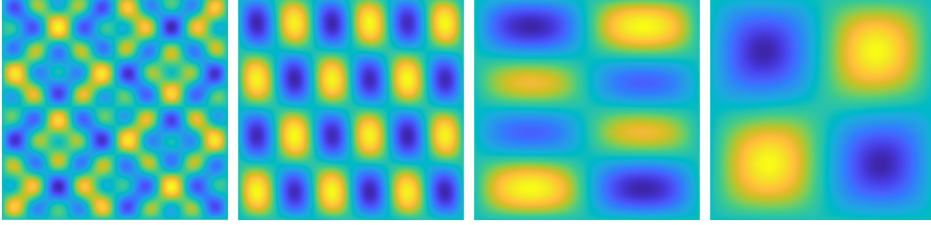


Figure 10: Snapshots of the phase variable ϕ at $t=0, 1, 6, 16$ for Example 5.

Example 6. In this case, we set the physical parameters as $a_0 = 1$, $b_0 = 0.025$, and $\Omega = [0, 128]^2$. The initial data ϕ is randomly generated as $\phi = \phi_0 + 0.01 \text{rand}(x, y)$, where $\phi_0 = 0.06$ and $\text{rand}(x, y)$ is a uniformly distributed random number between -1 and 1 . We use the following numerical settings to solve the PFC model: $\alpha = 10^{-6}$, $N_x = N_y = 256$, and $\Delta t = 1$. In Fig.11, we present the evolution of the density field ϕ calculated at $t = 100, 500, 1000, 2000$, which is in good agreement with the results published in [32]. The evolution of r_n is shown in Fig.12. It is observed that the value of r_n is close to 1, indicating the numerical consistency between the modified system and the original system.

Example 7. We simulate the growth of crystals in a supercooled liquid using the following expression to define the crystallites:

$$\phi_0(x_l, y_l) = \phi_0 + C_1 \left(\cos \left(\frac{C_2}{\sqrt{3}} y_l \right) \cos(C_2 x_l) - 0.5 \cos \left(\frac{2C_2}{\sqrt{3}} y_l \right) \right), \quad l = 1, 2, 3. \quad (121)$$

where x_l and y_l define a local system of Cartesian coordinates oriented with the crystallite lattice. The model parameters ϕ_0 , C_1 , and C_2 are set to $\phi_0 = 0.285$, $C_1 = 0.446$, and $C_2 = 0.66$, respectively. To generate the initial configuration, we place three perfect crystallites in small square patches located at $(350, 400)$, $(200, 200)$, and $(600, 300)$, each with a side length of 40. This configuration is similar to the numerical examples found in [32]. To generate crystallites with different orientations, we use the following affine transformation to produce a rotation given by three different angles $\theta = -\frac{\pi}{4}, 0, \frac{\pi}{4}$ respectively:

$$x_l(x, y) = x \sin(\theta) + y \cos(\theta), \quad y_l(x, y) = -x \cos(\theta) + y \sin(\theta). \quad (122)$$

In this simulation, we select the following parameters: $\epsilon = 0.25$, $M = 1$, $S = 0.1$, $\lambda = 0.001$, $\Omega = [0, 800]^2$, $N_x = N_y = 512$, and $\Delta t = 0.05$. Fig.14 illustrates the evolution of the phase transition behavior at different times

$t = 0, 25, 250, 800$. The results agree with the published findings in [32]. Fig.13 presents the evolution of r_n . It is evident that the value of r_n is close to 1, indicating the numerical consistency between the modified system and the original system.

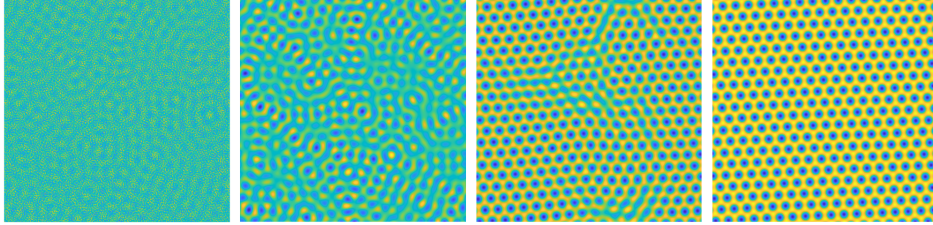


Figure 11: Snapshots of the phase variable ϕ at $t=100, 500, 1000, 2000$ for Example 6.

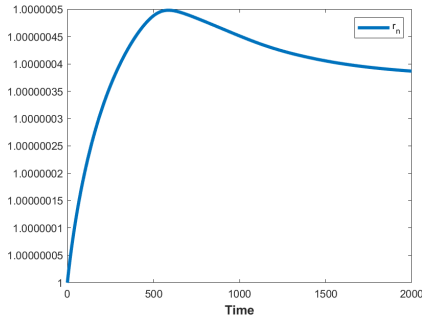


Figure 12: The evolution of r_n for Example 6.

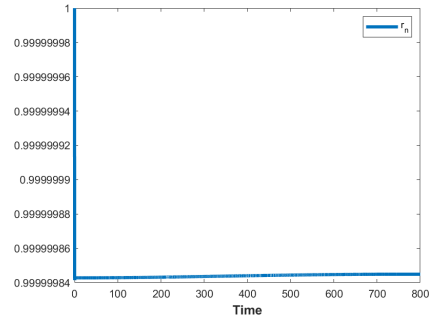


Figure 13: The evolution of r_n for Example 7.

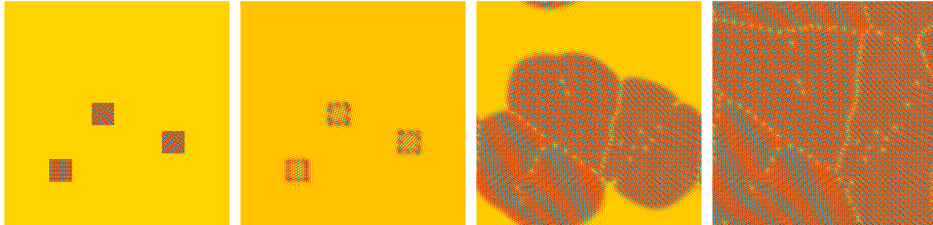


Figure 14: Snapshots of the phase variable ϕ at $t=0, 25, 250, 800$ for Example 7.

In the last example, we investigate the diblock copolymer model using the CSAV method. The free energy of the model is given by:

$$\mathcal{E} = \int_{\Omega} \frac{\varepsilon^2}{2} |\nabla \phi|^2 + \frac{1}{4} (\phi^2 - 1)^2 dx + \frac{\sigma}{2} \int_{\Omega} \int_{\Omega} G(\mathbf{x} - \mathbf{y}) (\phi(\mathbf{x}) - \hat{\phi}_0) (\phi(\mathbf{y}) - \hat{\phi}_0) dx dy \quad (123)$$

with σ representing a parameter for the nonlocal interaction strength and the mobility operator defined as $\mathcal{G} = -\lambda \Delta$. In this formulation, G corresponds to the Green's function satisfying $\Delta G(\mathbf{x} - \mathbf{y}) = -\delta(\mathbf{x} - \mathbf{y})$ with periodic boundary

conditions, where δ denotes the Dirac delta function. The general gradient flow model in (2) is specifically applied to the phase-field diblock copolymer model, which can be expressed as:

$$\phi_t = \lambda \left[\Delta\mu - \sigma \left(\phi - \hat{\phi}_0 \right) \right] \quad (124)$$

$$\mu = -\epsilon^2 \Delta\phi + \phi^3 - \phi. \quad (125)$$

The modified system is

$$\phi_t = \lambda \left[\Delta\mu - \sigma \left(\phi - \hat{\phi}_0 \right) \right], \quad (126)$$

$$\mu = -\epsilon^2 \Delta\phi + s\phi + r(\phi^3 - (s+1)\phi), \quad (127)$$

$$\frac{dr}{dt} = \alpha \left(-\frac{dE_{di0}(\phi)}{dt} + r \int_{\Omega} (\phi^3 - (s+1)\phi) \phi_t d\Omega \right). \quad (128)$$

where $E_{di0}(\phi) = \int_{\Omega} \left(\frac{1}{4}(\phi^2 - 1)^2 - \frac{s}{2}\phi^2 \right) d\Omega$.

The Second-order CN scheme is the following,

$$\frac{\phi^{n+1} - \phi^n}{\Delta t} = \lambda \Delta \mu^{n+\frac{1}{2}} - \lambda \sigma (\phi^{n+\frac{1}{2}} - \hat{\phi}_0), \quad (129)$$

$$\mu^{n+\frac{1}{2}} = -\epsilon^2 \Delta \phi^{n+\frac{1}{2}} + s\phi^{n+\frac{1}{2}} + \bar{r}^{n+\frac{1}{2}} \left((\bar{\phi}^{n+\frac{1}{2}})^3 - (s+1)\bar{\phi}^{n+\frac{1}{2}} \right), \quad (130)$$

$$\frac{r^{n+1} - r^n}{\Delta t} = \alpha \left(-\frac{E_{di0}(\phi^{n+1}) - E_{di0}(\phi^n)}{\Delta t} + \bar{r}^{n+\frac{1}{2}} \int_{\Omega} \left((\bar{\phi}^{n+\frac{1}{2}})^3 - (s+1)\bar{\phi}^{n+\frac{1}{2}} \right) \frac{\phi^{n+1} - \phi^n}{\Delta t} d\Omega \right). \quad (131)$$

Example 8. In this example, we investigate the phase separation dynamics known as spinodal decomposition using the CSAV scheme. We set the initial condition as the randomly perturbed concentration field, given by:

$$\phi(x, y, t = 0) = \bar{\phi}_0 + 0.001 \text{rand}(x, y),$$

where the $\text{rand}(x, y)$ represents the random number in $[-1, 1]$ that follows the normal distribution. We set the numerical parameters $\delta t = 0.001$ and $N_x = N_y = 256$. The model parameters are set as $\sigma = 100$, $\epsilon = 0.02$.

In Fig.15, we present the numerical results for the initial value $\bar{\phi}_0 = 0$. Snapshots of the phase field variable ϕ are taken at different time instances: $t = 0.05, 0.2, 0.5$, and 20 , which are in good agreement with the results in [33]. Fig.17 shows the evolution of r_n over time. It can be seen that the value of r_n remains close to 1 throughout the simulation. This indicates the numerical consistency between the modified system and the original system.

In Fig.16, we consider a different initial condition with $\bar{\phi}_0 = 0.3$. Snapshots of the phase field variable ϕ are captured at various time steps: $t = 0.05, 0.2, 0.5$, and 20 , which are in good agreement with the results in [33]. Fig.18 illustrates the evolution of r_n over time. The plot shows that the value of r_n remains close to 1 throughout the simulation, indicating the numerical consistency between the modified system and the original system.

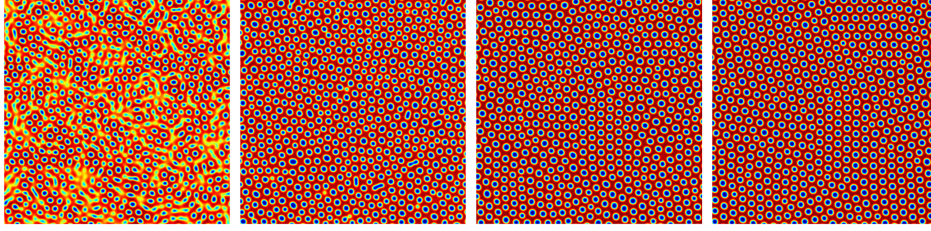


Figure 15: Snapshots of the phase variable ϕ at $t=0.05, 0.2, 0.5, 20$ when $\bar{\phi}_0 = 0$ for Example 8.

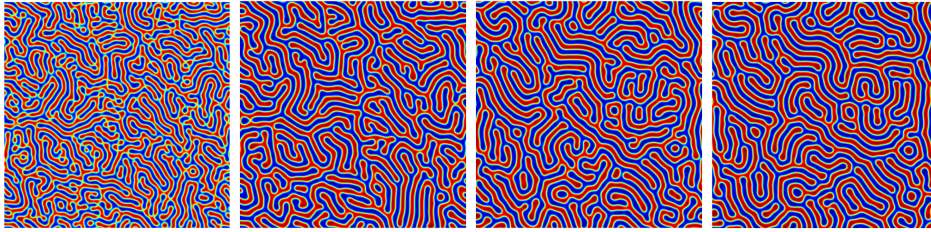


Figure 16: Snapshots of the phase variable ϕ at $t=0.05, 0.2, 0.5, 20$ when $\bar{\phi}_0 = 0.3$ for Example 8.

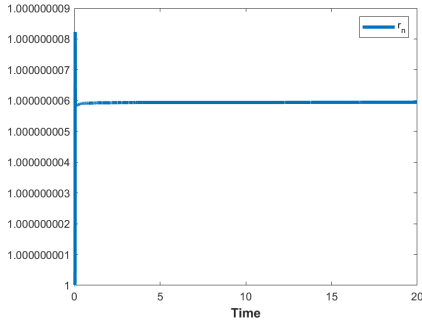


Figure 17: The evolution of r_n when $\bar{\phi}_0 = 0$ for Example 8.

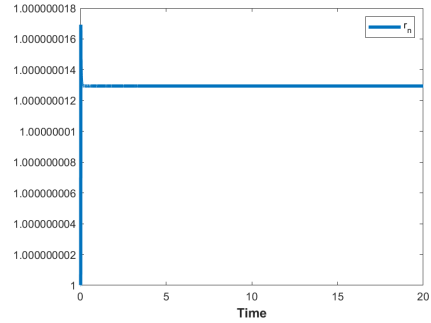


Figure 18: The evolution of r_n when $\bar{\phi}_0 = 0.3$ for Example 8.

6. Conclusions

In this paper, we propose a constant scalar auxiliary variable (CSAV) approach that effectively addresses the issue of inconsistency. We introduce a stabilization parameter (α) in the ODE for the scalar variable to slow down the change of the constant scalar variable, ensuring consistency between the original system and the modified system after numerical discretization. Extensive numerical simulations are carried out to show the accuracy and stability of the proposed method.

Acknowledgments

X.-P. Wang acknowledges support from the National Natural Science Foundation of China (NSFC) (No. 12271461), the key project of NSFC (No. 12131010), Shenzhen Science and Technology Innovation Program (Grant: C10120230046), the Hetao Shenzhen-Hong Kong Science and Technology Innovation Cooperation Zone Project (No.HZQSW-S-KCCYB-2024016) and the University Development Fund from The Chinese University of Hong Kong, Shenzhen (UDF01002028).

Appendix

Lemma 1 (Discrete Gronwall Lemma). Let y^k, h^k, g^k, f^k be four nonnegative sequences satisfying

$$y^n + \Delta t \sum_{k=0}^n h^k \leq B + \Delta t \sum_{k=0}^n (g^k y^k + f^k) \quad \text{with} \quad \Delta t \sum_{k=0}^{T/\Delta t} g^k \leq M, \forall 0 \leq n \leq T/\Delta t. \quad (132)$$

We assume $\Delta t g^k < 1$ and let $\sigma = \max_{0 \leq k \leq T/\Delta t} (1 - \Delta t g^k)^{-1}$. Then

$$y^n + \Delta t \sum_{k=1}^n h^k \leq \exp(\sigma M) \left(B + \Delta t \sum_{k=0}^n f^k \right), \quad \forall n \leq T/\Delta t. \quad (133)$$

Lemma 2 (Young inequality).

$$ab \leq \varepsilon a^p + C(\varepsilon) b^q, \quad a, b, \varepsilon > 0, \quad \frac{1}{p} + \frac{1}{q} = 1, \quad C(\varepsilon) = (\varepsilon p)^{-\frac{q}{p}} q^{-1}. \quad (134)$$

Let $\phi(t) = \phi(x, t)$ be the solution of the system (37)-(39) and $\phi^n = \phi^n(x)$, r^n be the solution of the discrete system (50)-(52). Denote $z^{n+1} = |r^{n+1} - 1|$ and $e^{n+1} = \phi^{n+1} - \phi(t^{n+1})$. We have the following theorem.

Theorem 5. Assume that $\phi(t_0) \in \mathbf{H}^2(\Omega)$, $\phi^n \in \mathbf{H}^2(\Omega)$, $\phi_t \in \mathbf{L}^\infty(0, T; \mathbf{L}^2(\Omega))$, $\phi_{tt} \in \mathbf{L}^2(0, T; \mathbf{L}^2(\Omega))$, We then have

(i). $\lim_{\alpha \rightarrow 0} |r^n - 1| = 0$.

(ii). $\lim_{\Delta t \rightarrow 0} \frac{1}{\alpha} |r^n - 1| = 0$.

(iii). For all $n \leq T/\Delta t$, $\exists \alpha_0, \forall \alpha \leq \alpha_0$, we have

$$\frac{1}{2} \|\nabla e^n\|^2 + \frac{s}{2} \|e^n\|^2 \leq C \exp((1 - C\Delta t)^{-1} C t^n) \left(\Delta t^2 \int_0^{t_n} \|\phi_{tt}(s)\|^2 + \|\phi_t(s)\|^2 ds + \Delta t \alpha \right). \quad (135)$$

The constant C is dependent on $T, \phi(t_0), |\Omega|, \|\phi\|_{\mathbf{L}^\infty(0, T; W^{1, \infty}(\Omega))}, \|\phi_t\|_{\mathbf{L}^\infty(0, T; \mathbf{L}^2(\Omega))}$.

Proof: Let $w^{n+1} = \mu^{n+1} - \mu(t^{n+1})$. Because $\phi(t_0) \in \mathbf{H}^2(\Omega)$, we know $\phi(t) \in \mathbf{C}([0, T]; \mathbf{H}^2)$ ([34], Theorem 2.6). $\phi(t), \phi^n \in \mathbf{H}^2(\Omega) \not\subseteq \mathbf{L}^\infty(\Omega)$, we can find a constant C such that $|g(\phi)|, |g'(\phi)|, |g(\phi^n)|, |g'(\phi^n)|, |E_0(\phi)|, |E_0(\phi^n)| \leq C$. Let $z^{n+1} = |r^{n+1} - 1|$, by the absolute value inequality, we have

$$\begin{aligned} z^{n+1} - z^n &= (|r^{n+1} - 1| - |r^n - 1|) \leq |(r^{n+1} - 1) - (r^n - 1)| \\ &= \alpha \left| - (E_0(\phi^{n+1}) - E_0(\phi^n)) + (r^n - 1) \int_{\Omega} g(\phi^n)(\phi^{n+1} - \phi^n) d\Omega + \int_{\Omega} g(\phi^n)(\phi^{n+1} - \phi^n) d\Omega \right| \\ &\leq \alpha \left| (E_0(\phi^{n+1}) - E_0(\phi^n)) - \int_{\Omega} g(\phi^n)(\phi^{n+1} - \phi^n) d\Omega \right| + \alpha z^n \int_{\Omega} |g(\phi^n)(\phi^{n+1} - \phi^n)| d\Omega \end{aligned} \quad (136)$$

For the first term, because $E_0(\phi^{n+1}) = \int_{\Omega} F(\phi^{n+1}) d\Omega$, and $F'(\phi^{n+1}) = g(\phi^{n+1})$, we can obtain

$$\begin{aligned} &\left| (E_0(\phi^{n+1}) - E_0(\phi^n)) - \int_{\Omega} g(\phi^n)(\phi^{n+1} - \phi^n) d\Omega \right| \\ &= \left| \int_{\Omega} F(\phi^{n+1}) - F(\phi^n) - g(\phi^n)(\phi^{n+1} - \phi^n) d\Omega \right| \\ &= \left| \int_{\Omega} g(\xi_1)(\phi^{n+1} - \phi^n) - g(\phi^n)(\phi^{n+1} - \phi^n) d\Omega \right| \\ &= \left| \int_{\Omega} (g(\xi_1) - g(\phi^n))(\phi^{n+1} - \phi^n) d\Omega \right| \\ &= \left| \int_{\Omega} g'(\xi_2)(\xi_1 - \phi^n)(\phi^{n+1} - \phi^n) d\Omega \right| \\ &\leq C \int_{\Omega} |\xi_1 - \phi^n| |\phi^{n+1} - \phi^n| d\Omega \end{aligned} \quad (137)$$

Because ξ_1 is between ϕ^{n+1} and ϕ^n , and $\phi^n \in \mathbf{H}^2(\Omega)$, we can get

$$|\xi_1 - \phi^n| \leq |\phi^{n+1} - \phi^n| = \Delta t |\Delta \phi^{n+1} - s\phi^{n+1} - r^n g(\phi^n)| \leq C \Delta t \quad (138)$$

where it is easy to get $r^n \in L^\infty(0, T)$ because of $\phi^n \in \mathbf{H}^2(\Omega)$. By combining (136), (137) and (138), we can get

$$z^{n+1} - z^n \leq C \alpha \Delta t z^n + C \alpha \Delta t^2 \quad (139)$$

Taking the summation of (136) for n from 0 to m ,

$$z^{m+1} \leq C \Delta t \alpha \sum_{n=0}^m z^n + C \Delta t \alpha \quad (140)$$

Using the discrete Gronwall lemma, we can get

$$z^m \leq C \exp((1 - \Delta t \alpha C)^{-1} t^m C \alpha) \alpha \Delta t \quad (141)$$

(i) and (ii) then follow from the above inequality. We now prove the inequality (135).

The equations for the errors are written as

$$e^{n+1} - e^n = -\Delta t w^{n+1} - T_1^n, \quad (142)$$

$$w^{n+1} = -\Delta e^{n+1} + s e^{n+1} + (r^n - 1)g(\phi^n) + (g(\phi^n) - g(\phi(t^n))) + T_2^n, \quad (143)$$

$$T_1^n = \phi(t^{n+1}) - \phi(t^n) - \Delta t \phi_t(t^{n+1}) = \int_{t^n}^{t^{n+1}} (t^n - s) \phi_{tt}(s) ds \quad (144)$$

$$T_2^n = g(\phi(t^n)) - g(\phi(t^{n+1})) \quad (145)$$

Multiplying (142) with w^{n+1} , (143) with $e^{n+1} - e^n$, then summing up the two equations, we get

$$\begin{aligned} & \frac{s}{2} \left(\|e^{n+1}\|^2 - \|e^n\|^2 \right) + \frac{1}{2} \left(\|\nabla e^{n+1}\|^2 - \|\nabla e^n\|^2 \right) + \frac{s}{2} \left(\|e^{n+1} - e^n\|^2 \right) + \frac{1}{2} \left(\|\nabla e^{n+1} - \nabla e^n\|^2 \right) + \Delta t \|w^{n+1}\|^2 \\ & = (1 - r^n) \int_{\Omega} g(\phi^n) (e^{n+1} - e^n) d\Omega - \int_{\Omega} (g(\phi^n) - g(\phi(t^n))) (e^{n+1} - e^n) d\Omega - (T_1^n, w^{n+1}) \\ & - (T_2^n, e^{n+1} - e^n) \end{aligned} \quad (146)$$

We have the following estimates:

$$\begin{aligned} & (1 - r^n) \int_{\Omega} g(\phi^n) (e^{n+1} - e^n) d\Omega \\ & \leq |1 - r^n| \int_{\Omega} |g(\phi^n)| |e^{n+1} - e^n| d\Omega \\ & \leq |1 - r^n| \Delta t \int_{\Omega} \left(|g(\phi^n)| |w^{n+1}| + |g(\phi^n)| \left| \frac{T_1^n}{\Delta t} \right| \right) d\Omega \\ & \leq |1 - r^n| \Delta t \left(\frac{1}{2} \|w^{n+1}\|^2 + \|g(\phi^n)\|^2 + \frac{1}{2\Delta t^2} \|T_1^n\|^2 \right) \\ & \leq \frac{|1 - r^n| \Delta t}{2} \|w^{n+1}\|^2 + |1 - r^n| \Delta t \|g(\phi^n)\|^2 + \frac{|1 - r^n|}{2\Delta t} \|T_1^n\|^2 \\ & \leq \frac{\Delta t}{4} \|w^{n+1}\|^2 + |1 - r^n| \Delta t \|g(\phi^n)\|^2 + \frac{|1 - r^n|}{2\Delta t} \|T_1^n\|^2 \end{aligned} \quad (147)$$

$$\begin{aligned} & \int_{\Omega} (g(\phi^n) - g(\phi(t^n))) (e^{n+1} - e^n) d\Omega \\ & \leq \frac{\Delta t}{4} \|w^{n+1}\|^2 + C \Delta t \|(g(\phi^n) - g(\phi(t^n)))\|^2 + \frac{C}{\Delta t} \|T_1^n\|^2 \\ & \leq \frac{\Delta t}{4} \|w^{n+1}\|^2 + C \Delta t \|e^n\|^2 + \frac{C}{\Delta t} \|T_1^n\|^2 \end{aligned} \quad (148)$$

Note that $\lim_{\alpha \rightarrow 0} |r^{n+1} - 1| = 0$, so $\exists \alpha_0, \forall \alpha < \alpha_0, |r^{n+1} - 1| < 1/2$, so $\frac{|1 - r^n| \Delta t}{2} \|w^{n+1}\|^2 \leq \frac{\Delta t}{4} \|w^{n+1}\|^2$ in (147).

For the truncation errors, we have the following estimates:

$$\begin{aligned}
\|T_1^n\|^2 &= \int_{\Omega} \left| \int_{t^n}^{t^{n+1}} (t^n - s) \phi_{tt}(s) ds \right|^2 d\Omega \\
&\leq \int_{\Omega} \left| \int_{t^n}^{t^{n+1}} |t^n - s| |\phi_{tt}(s)| ds \right|^2 d\Omega \\
&\leq \int_{\Omega} \int_{t^n}^{t^{n+1}} |t^n - s|^2 ds \int_{t^n}^{t^{n+1}} |\phi_{tt}(s)|^2 ds d\Omega \\
&\leq \Delta t^3 \int_{t^n}^{t^{n+1}} \|\phi_{tt}(s)\|^2 ds
\end{aligned} \tag{149}$$

$$\begin{aligned}
\|T_2^n\|^2 &= \int_{\Omega} |g(\phi(t^n)) - g(\phi(t^{n+1}))|^2 d\Omega \\
&\leq \int_{\Omega} |g'(\xi)|^2 |\phi(t^{n+1}) - \phi(t^n)|^2 d\Omega \\
&\leq C \int_{\Omega} \left| \int_{t^n}^{t^{n+1}} \phi_t(s) ds \right|^2 d\Omega \\
&\leq C\Delta t \int_{t^n}^{t^{n+1}} \|\phi_t(s)\|^2 ds
\end{aligned} \tag{150}$$

Therefore,

$$(T_1^n, w^{n+1}) \leq \frac{\Delta t}{4} \|w^{n+1}\|^2 + \frac{C}{\Delta t} \|T_1^n\|^2 \leq \frac{\Delta t}{4} \|w^{n+1}\|^2 + C\Delta t^2 \int_{t^n}^{t^{n+1}} \|\phi_{tt}(s)\|^2 ds \tag{151}$$

$$\begin{aligned}
(T_2^n, e^{n+1} - e^n) &\leq \Delta t \left(|w^{n+1}| + \left| \frac{T_1^n}{\Delta t} \right|, |T_2^n| \right) \\
&\leq \frac{\Delta t}{4} \|w^{n+1}\|^2 + C\Delta t^2 \int_{t^n}^{t^{n+1}} \|\phi_{tt}(s)\|^2 ds + C\Delta t^2 \int_{t^n}^{t^{n+1}} \|\phi_t(s)\|^2 ds
\end{aligned} \tag{152}$$

Combining (146), (147), (148), (149), (150), (151) and (152), we obtain

$$\begin{aligned}
&\frac{s}{2} \left(\|e^{n+1}\|^2 - \|e^n\|^2 \right) + \frac{1}{2} \left(\|\nabla e^{n+1}\|^2 - \|\nabla e^n\|^2 \right) \\
&\leq |1 - r^n| \Delta t \|g(\phi^n)\|^2 + C\Delta t^2 \int_{t^n}^{t^{n+1}} \|\phi_{tt}(s)\|^2 ds + C\Delta t \|e^n\|^2 + C\Delta t^2 \int_{t^n}^{t^{n+1}} \|\phi_t(s)\|^2 ds \\
&\leq C \exp((1 - \Delta t \alpha C)^{-1} t^n C \alpha) \alpha \Delta t^2 + C\Delta t^2 \int_{t^n}^{t^{n+1}} \left(\|\phi_{tt}(s)\|^2 + \|\phi_t(s)\|^2 \right) ds + C\Delta t \left(\|e^n\|^2 + \|\nabla e^n\|^2 \right)
\end{aligned} \tag{153}$$

Taking the summation of (153) for n from 0 to m ,

$$\begin{aligned}
& \frac{s}{2} \|e^{m+1}\|^2 + \frac{1}{2} \|\nabla e^{m+1}\|^2 \\
& \leq C\alpha\Delta t^2 \sum_{n=0}^m \exp((1 - \Delta t\alpha C)^{-1}t^n C\alpha) + C\Delta t^2 \sum_{n=0}^m \int_{t^n}^{t^{n+1}} \left(\|\phi_{tt}(s)\|^2 + \|\phi_t(s)\|^2 \right) ds \\
& + C\Delta t \sum_{n=0}^m \left(\|e^n\|^2 + \|\nabla e^n\|^2 \right)
\end{aligned} \tag{154}$$

Because $\lim_{\alpha \rightarrow 0} \exp((1 - \Delta t C \alpha)^{-1} t^n C \alpha) = 1$, $\exists \alpha_0, \forall \alpha \leq \alpha_0, \exp((1 - \Delta t C \alpha)^{-1} t^n C \alpha) < C$. Then we can conclude the proof by applying the discrete Gronwall's inequality to the above.

References

- [1] J. Shen, J. Xu, J. Yang, The scalar auxiliary variable (sav) approach for gradient flows, *Journal of Computational Physics* 353 (2018) 407–416.
- [2] D. M. Anderson, G. B. McFadden, A. A. Wheeler, Diffuse-interface methods in fluid mechanics, *Annual review of fluid mechanics* 30 (1998) 139–165.
- [3] M. Gao, X.-P. Wang, A gradient stable scheme for a phase field model for the moving contact line problem, *Journal of Computational Physics* 231 (2012) 1372–1386.
- [4] K. Elder, M. Katakowski, M. Haataja, M. Grant, Modeling elasticity in crystal growth, *Physical review letters* 88 (2002) 245701.
- [5] F. M. Leslie, Theory of flow phenomena in liquid crystals, in: *Advances in liquid crystals*, volume 4, Elsevier, 1979, pp. 1–81.
- [6] L. Luo, X.-P. Wang, X.-C. Cai, An efficient finite element method for simulation of droplet spreading on a topologically rough surface, *Journal of Computational Physics* 349 (2017) 233–252.
- [7] M. E. Gurtin, D. Polignone, J. Vinals, Two-phase binary fluids and immiscible fluids described by an order parameter, *Mathematical Models and Methods in Applied Sciences* 6 (1996) 815–831.
- [8] S. M. Allen, J. W. Cahn, A microscopic theory for antiphase boundary motion and its application to antiphase domain coarsening, *Acta metallurgica* 27 (1979) 1085–1095.
- [9] J. W. Cahn, J. E. Hilliard, Free energy of a nonuniform system. i. interfacial free energy, *The Journal of chemical physics* 28 (1958) 258–267.

- [10] J. Villain, Continuum models of crystal growth from atomic beams with and without desorption, *Journal de physique I* 1 (1991) 19–42.
- [11] A. Baskaran, J. S. Lowengrub, C. Wang, S. M. Wise, Convergence analysis of a second order convex splitting scheme for the modified phase field crystal equation, *SIAM Journal on Numerical Analysis* 51 (2013) 2851–2873.
- [12] C. M. Elliott, A. Stuart, The global dynamics of discrete semilinear parabolic equations, *SIAM journal on numerical analysis* 30 (1993) 1622–1663.
- [13] D. J. Eyre, Unconditionally gradient stable time marching the cahn-hilliard equation, *MRS online proceedings library (OPL)* 529 (1998) 39.
- [14] J. Shen, X. Yang, Numerical approximations of allen-cahn and cahn-hilliard equations, *Discrete Contin. Dyn. Syst* 28 (2010) 1669–1691.
- [15] J. Zhu, L.-Q. Chen, J. Shen, V. Tikare, Coarsening kinetics from a variable-mobility cahn-hilliard equation: Application of a semi-implicit fourier spectral method, *Physical Review E* 60 (1999) 3564.
- [16] X. Wang, L. Ju, Q. Du, Efficient and stable exponential time differencing runge–kutta methods for phase field elastic bending energy models, *Journal of Computational Physics* 316 (2016) 21–38.
- [17] S. M. Cox, P. C. Matthews, Exponential time differencing for stiff systems, *Journal of Computational Physics* 176 (2002) 430–455.
- [18] X. Yang, Linear, first and second-order, unconditionally energy stable numerical schemes for the phase field model of homopolymer blends, *Journal of Computational Physics* 327 (2016) 294–316.
- [19] X. Yang, L. Ju, Efficient linear schemes with unconditional energy stability for the phase field elastic bending energy model, *Computer Methods in Applied Mechanics and Engineering* 315 (2017) 691–712.
- [20] J. Shen, J. Xu, J. Yang, A new class of efficient and robust energy stable schemes for gradient flows, *SIAM Review* 61 (2019) 474–506.
- [21] W. Chen, X. Wang, Y. Yan, Z. Zhang, A second order bdf numerical scheme with variable steps for the cahn–hilliard equation, *SIAM Journal on Numerical Analysis* 57 (2019) 495–525.
- [22] Z. Zhang, Z. Qiao, An adaptive time-stepping strategy for the cahn-hilliard equation, *Communications in Computational Physics* 11 (2012) 1261–1278.

- [23] Q. Cheng, C. Liu, J. Shen, A new lagrange multiplier approach for gradient flows, *Computer Methods in Applied Mechanics and Engineering* 367 (2020) 113070.
- [24] M. Jiang, Z. Zhang, J. Zhao, Improving the accuracy and consistency of the scalar auxiliary variable (sav) method with relaxation, *Journal of Computational Physics* 456 (2022) 110954.
- [25] Y. Zhang, J. Shen, A generalized sav approach with relaxation for dissipative systems, *Journal of Computational Physics* 464 (2022) 111311.
- [26] Z. Liu, X. Li, The exponential scalar auxiliary variable (e-sav) approach for phase field models and its explicit computing, *SIAM Journal on Scientific Computing* 42 (2020) B630–B655.
- [27] C. Chen, X. Yang, Highly efficient and unconditionally energy stable semi-discrete time-marching numerical scheme for the two-phase incompressible flow phase-field system with variable-density and viscosity, *Science China Mathematics* 65 (2022) 2631–2656.
- [28] J. Zhang, C. Zhang, X.-P. Wang, An efficient unconditional energy stable scheme for the simulation of droplet formation; journal of computational physics, *Journal of Computational Physics* 507 (2024) 112974.
- [29] L. Chen, J. Zhao, X. Yang, Regularized linear schemes for the molecular beam epitaxy model with slope selection, *Applied Numerical Mathematics* 128 (2018) 139–156.
- [30] Q. Cheng, J. Shen, Multiple scalar auxiliary variable (msav) approach and its application to the phase-field vesicle membrane model, *SIAM Journal on Scientific Computing* 40 (2018) A3982–A4006.
- [31] C. Xu, T. Tang, Stability analysis of large time-stepping methods for epitaxial growth models, *SIAM Journal on Numerical Analysis* 44 (2006) 1759–1779.
- [32] X. Li, J. Shen, Stability and error estimates of the sav fourier-spectral method for the phase field crystal equation, *Advances in Computational Mathematics* 46 (2020) 1–20.
- [33] J. Zhang, C. Chen, X. Yang, Efficient and energy stable method for the cahn-hilliard phase-field model for diblock copolymers, *Applied Numerical Mathematics* 151 (2020) 263–281.
- [34] J. Shen, J. Xu, Convergence and error analysis for the scalar auxiliary variable (sav) schemes to gradient flows, *SIAM Journal on Numerical Analysis* 56 (2018) 2895–2912.